A Longitudinal MRI Study of Histopathologically Defined Hypointense Multiple Sclerosis Lesions

Andreas Bitsch, MD,[1] Tanja Kuhlmann, MD,[2] Christine Stadelmann, MD,[2] Hans Lassmann, MD,[3] Claudia Lucchinetti, MD,[4] and Wolfgang Brück, MD[2]

Severe tissue destruction is the presumed histopathological correlate of hypointense multiple sclerosis (MS) lesions. In this study we correlated changes of lesion hypointensity over time with initial histopathological features in 14 biopsied MS lesions. The extent of hypointensity increased in initially demyelinated plaques and decreased in remyelinating lesions. The initial axonal loss determined the increase of hypointensity over time. In conclusion, both axonal loss and demyelinating activity determine the evolution of hypointensity over time.

Ann Neurol 2001;49:793–796

Axonal loss in multiple sclerosis (MS) mainly contributes to clinical disability and occurs early in lesion development.[1–3] In standard magnetic resonance imaging (MRI), cerebral atrophy and T1 hypointense lesions ("black holes") are thought to reflect axonal loss. In combined histopathological and MRI studies, axonal loss appeared to be the correlate of lesion hypointensity.[4,5] N-acetyl-aspartate (NAA), an in vivo marker of axons, was strongly decreased in hypointense lesions.[6] Magnetization transfer ratio (MTR) also correlated with axonal density in a comparative morphological-radiological study.[7] Correlative MTR-MRI studies revealed a clear association between these two markers and their predictive value for disease progression or clinical disability in MS.[8–12] However, the extent of hypointensity of an MS lesion is known to change over time.[13] A strongly decreased magnetization transfer ratio (MTR) and a long-lasting ring enhancement are predictive of persistent hypointensity.[13] However, the histopathological determinants affecting long-term development of lesion hypointensity have not been elucidated so far. In the present study, we longitudinally analyzed T1 lesion hypointensity of biopsy-defined inflammatory demyelinating central nervous system (CNS) lesions.

From the [1]Abteilung Neurologie, Georg-August-Universität, Göttingen, [2]Institut für Neuropathologie, Charité, Campus Virchow-Klinikum, Berlin, Germany, [3]Institut für Hirnforschung, Abt. Neuroimmunologie, Vienna, Austria, and [4]Department of Neurology, Mayo Clinic, Rochester, MN

Received Nov 20, 2000 and in revised form Feb 16, 2001. Accepted for publication Feb 17, 2001.

Address correspondence to Dr Brück, Institut für Neuropathologie, Charité, Campus Virchow-Klinikum, Augustenburger Platz 1, 13353 Berlin, Germany. E-mail: wolfgang.brueck@charite.de

Materials and Methods

Patients

Brain biopsy specimen of patients who had been biopsied in the very early course of their disease were collected at the Institute of Neuropathology of the Charité, Berlin, Germany. These biopsies were performed to exclude treatable conditions other than MS. None of the authors was involved in decision making for biopsy. The attending physician obtained informed consent from each patient prior to biopsy.

We analyzed 14 biopsies from 13 patients (9 women, 4 men, age 20–52 years, median: 36 years; Table). Based on clinical follow-up data, 10 patients had a relapsing-remitting and 3 had a primary progressive disease course. At present, diagnosis is definite in 7 patients and probable in 6 patients according to Poser's criteria.[14]

Neuropathology

Paraffin-embedded tissue was used. Routine neuropathological stains (H & E, Luxol-Fast Blue myelin stain, Bielschowsky's silver impregnation for axons) were applied as well as immunocytochemistry for the following markers: antimyelin basic protein (MBP, Boehringer Mannheim, Mannheim, Germany), antiproteolipid protein (PLP, Dr. Piddlesden, University of Cardiff, UK), antimyelin oligodendrocyte glycoprotein (MOG, Dr. Piddlesden), anti-KiMlP (macrophages/microglia, Dr. Radzun, University of Göttingen, Germany), anti-27E10 and anti-MRP14 (activated macrophages, BMA Biomedicals, August, Switzerland), anti-CD3 (T cells, Dako, Denmark), anti-CD8 (Dako, Denmark), and anti-amyloid precursor protein (APP; Boehringer Mannheim, Germany). An avidin biotin complex or an alkaline phosphatase/antialkaline phosphatase technique was used with the appropriate controls.

Biopsies were classified with respect to demyelinating activity and axonal loss as described in detail earlier.[3,15] *Active demyelinating lesions* (A) were diffusely infiltrated by macrophages containing myelin proteins as markers of recent myelin phagocytosis. *Remyelinating lesions* (R) were characterized by uniformly thin and irregularly arranged myelin sheaths. *Inactive demyelinated lesions* (I) were completely demyelinated without signs of active demyelination. Axonal loss was expressed as the percentage of axonal density inside the lesions compared to axonal density in the periplaque white matter (PPWM).[3]

MRI Analysis

All MRI scans were copies of the original scans that had been performed at local institutions near to the patient's place of residence. A baseline MRI scan close to biopsy was available for each patient (see Table). These were performed prior to biopsy in 12 patients and after biopsy in 2 patients (median: -4.5 days prior to biopsy, range -27–45 days). A total of 32 follow-up scans was available for analysis (median time after

Table. Baseline MRI Lesion Characteristics (n = 14) and Patients' Clinical Findings that led to Biopsy (n = 13)

Patient	Lesion size[a]	Gadolinium enhancement[b]	Clinical and paraclinical findings
1	>5 cm	Not known	Bilateral amaurosis, ataxia, normal CSF, bilateral large lesions
2	<2 cm	Open ring	Tetraparesis, stupor, OCB, confluent bilateral lesions
3	2–5 cm	Open ring	Hemiparesis, aphasia, OCB, bilateral enhancing lesions
4	>5 cm	Ring	Organic brain syndrome, hemiparesis, CSF normal, bilateral enhancing lesions
5	>5 cm	Nodular	Seizures, hemiparesis, aphasia, CSF: pleocytosis, bilateral enhancing lesions
6	2–5 cm	Nodular	Hemiparesis, ataxia, CSF normal, bilateral enhancing lesions
7 (1^{st})	2–5 cm	Homogeneous	Seizures, papilledema, CSF normal, bilateral confluent enhancing lesions
7 (2^{nd})	>5 cm	Ring	Progressive organic brain syndrome
8	2–5 cm	Ring	Vision loss, hemiparesis, ataxia, OCB, bilateral confluent hemispheric and cerebellar lesions
9	>5 cm	Nodular	Paraparesis, hemianopsia, CSF: pleocytosis (267/μl), large occipital lesion
10	>5 cm	Open ring	Stupor, aphasia, CSF normal, multiple cystic lesions right hemisphere
11	2–5 cm	Ring	Tetraparesis, CSF normal, bilateral confluent lesions including brain stem
12	2–5 cm	Ring	Hemiparesis, OCB, multiple periventricular lesions, one large left-hemispheric lesion
13	<2 cm	Nodular	Hemiparesis, CSF normal, one singular lesion right hemisphere

[a]Largest diameter of biopsied lesion on MRI (T2).
[b]Biopsied lesion; OCB (oligoclonal IgG bands).

biopsy: 323 days, range: 33–806 days). Lesion and white matter density was determined from MRI films with a transmission densitometer (X-rite 301) as described earlier.[4] Hypointensity on T1 scans was measured in five randomly selected areas inside the lesion and in five areas of the normal appearing white matter (NAWM) of the contralateral hemisphere. If the biopsy channel was visible, density measures were performed outside this region. Relative lesion hypointensity was calculated by dividing mean hypointensity of the lesion by mean hypointensity of the contralateral NAWM. Values larger than 1 indicate hypointensity of the lesion compared to NAWM.

Statistical evaluations were performed with the GraphPad PRISM™ software (version 2.0, GraphPad Software, Inc., San Diego, CA). Nonparametric tests were applied: Mann-Whitney tests for comparison of unpaired groups, Spearman rank correlation. In case of multiple comparisons, Bonferroni correction was performed.

Results

Microscopic evaluation revealed the typical features of MS, such as confluent demyelination and inflammatory infiltrates consisting of macrophages and lymphocytes. The determination of demyelinating activity showed 4 active demyelinating, 7 remyelinating, and 3 inactive demyelinated lesions. Axonal density was reduced in all but one lesion compared to the periplaque white matter (median 41%, range 0–71%; Fig 1a–c). During follow-up after biopsy, the relative lesion hy-

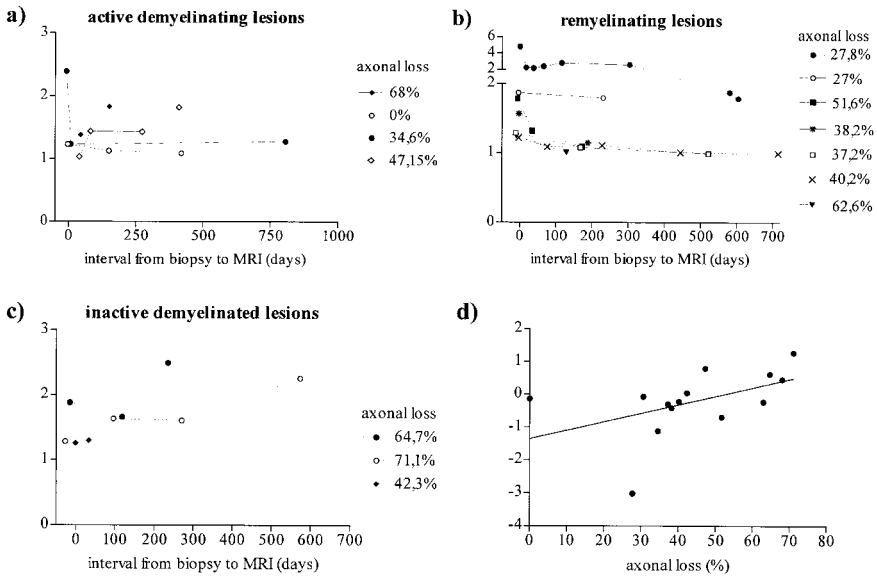

Fig 1. Longitudinal evolution of relative T1 hypointensity in active demyelinating (a), remyelinating (b), or inactive demyelinated (c) MS lesions. Axonal loss is given in percent of axonal density compared to the periplaque white matter. Relative T1 lesion hypointensity is calculated as the quotient of lesion hypointensity and intensity of the contralateral normal appearing white matter. (d) Correlation of axonal loss with the increase or decrease in relative lesion hypointensity over time. Axonal loss correlates with an increase in lesion hypointensity over time. Spearman rank correlation, r = 0.58, $p = 0.03$.

pointensity on MRI scans (T1) decreased in all remyelinating lesions and increased in all inactive demyelinated lesions (see Fig 1b,c; Fig 2). In active demyelinating lesions, the relative hypointensity either increased (n = 2) or decreased (n = 2) over time (see Fig 1a). The difference in lesion hypointensity between the initial and the last follow up scan was significantly lower in remyelinating (median −0.3) than in inactive demyelinated lesions (median +0.6; $p < 0.05$ after Bonferroni correction).

At biopsy, relative hypointensity (T1) inside the lesions did not correlate with axonal loss or the stage of demyelinating activity. Axonal loss was most prominent in inactive demyelinated lesions (median 65%), but compared to active demyelinating (41%) or remyelinating lesions (39%), this difference was not statistically significant. There was a significant connection between the evolution of lesion hypointensity over time and the initial extent of axonal loss (Spearman rank correlation, $r = 0.58$, $p = 0.03$). The higher the axonal loss was in the initial biopsy, the more hypointense the lesion became on follow-up scans (see Fig. 1d).

Fig 2. Sequential MRI scans of an inactive demyelinated lesion (a,b; arrows*). Lesion hypointensity increased over time (575 days; initial axonal loss 71.1%). In contrast, hypointensity of a remyelinating lesion decreased within 603 days (c,d;* arrows*; initial axonal loss 27.8%;* arrowhead *indicates biopsy channel).*

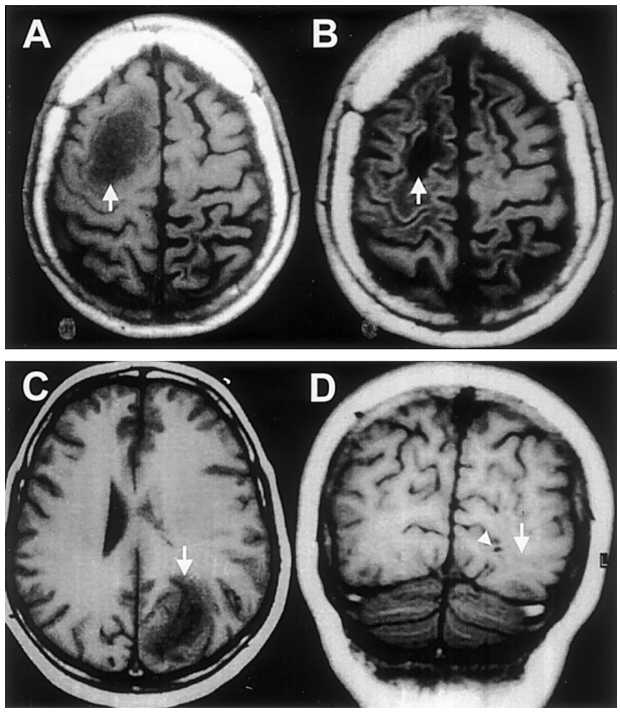

Discussion

The present study correlates long-term MRI development of MS plaques with initial histopathological features of the biopsied lesions. Our data confirm earlier evidence that hypointense MS lesions either become more or less hypointense over time.[13] The present study also indicates that the future evolution of hypointensity of an MS lesion depends on at least two features, the demyelinating activity of the lesion and the extent of axonal loss.

Severe initial axonal loss appears to be a potential predictor for the future increase of T1 hypointensity. In addition, completely demyelinated lesions showed an increase in hypointensity over time. In contrast, remyelinated lesions became less hypointense or even isointense over time. Although the low number of patients and the quality of imaging data limits our study, it may be speculated from the data that inactive demyelinated lesions rarely become remyelinated again. The decision, whether a lesion becomes remyelinated or not, seems to take place immediately following active demyelination. This may explain why active demyelinating lesions in our study became either less or more hypointense over time. Lesions may either proceed directly into remyelination or become inactive and stay demyelinated. Remyelination of MS lesions is known to occur early in plaque development.[16,17] The earlier remyelination starts, the more effective and complete it appears to be.[16] Remyelination may subsequently reduce the extracellular space, lead to compaction of the tissue, and finally result in a more isointense T1 signal. In completely demyelinated lesions, the failure of remyelination combined with ongoing axonal destruction may cause the increase in T1 hypointensity. In addition, it might be speculated that naked axons are particularly susceptible to irreversible damage by processes that may be noninflammatory.

Our data do not show a strict correlation between the grade of T1 hypointensity and the extent of axonal loss in the initial stage of lesion formation. Different factors such as active demyelination, edema, cellular infiltration, and astrogliosis may lead to increased extracellular free water and thus are prone to increase T1 hypointensity.[4,18] These so-called "acute black holes" may have a multifactorial origin in contrast to the permanent hypointense lesions, in which demyelination is complete and axonal loss may be the predominant underlying pathology. An acute black hole may thoroughly become isointense over time, which in view of our data may carefully be interpreted as an indirect sign of remyelination. This, however, remains to be confirmed. Only black holes that stay black holes over time seem to reflect an irreversible state of tissue destruction with both demyelination and axonal loss.

From the present study there is supportive evidence that marked axonal loss in an inactive demyelinated le-

sion is a potential predictor of an increase in hypointensity during the further lesion development. In radiological studies, this has also been shown for the initial T1 lesion load, but only partially for the degree of inflammatory activity.[19] Our findings may have implications not only for the understanding of lesion evolution and the meaning of T1 hypointensity but also for MRI as a surrogate outcome parameter for clinical studies. To date, only the volume and number of hypointense lesions have been introduced as an outcome measure.[20] In future studies, the evolution of increasing hypointensity in single lesions over time could serve as a marker of persistent tissue destruction. In contrast, resolving hypointensity may be interpreted as remyelination. Currently, there is an urgent need to establish markers of remyelination. Further studies with more patients will be needed to confirm our findings.

This study was supported by a grant from the Gemeinnützige Hertie-Stiftung (No. 2/540/99) and the United States Multiple Sclerosis Society (RG 3051-A-1). We gratefully acknowledge the support of many colleagues who provided biopsy specimen, MRI films, and clinical data of their patients.

References

1. De Stefano N, Matthews PM, Fu L, et al. Axonal damage correlates with disability in patients with relapsing-remitting multiple sclerosis. Results of a longitudinal magnetic resonance spectroscopy study. Brain 1998;121:1469–1477
2. Trapp BD, Peterson J, Ransohoff RM, et al. Axonal transection in the lesions of multiple sclerosis. New Engl J Med 1998;338: 278–285
3. Bitsch A, Schuchardt J, Bunkowski S, et al. Axonal injury in multiple sclerosis. Correlation with demyelination and inflammation. Brain 2000;123:1174–1183
4. Brück W, Bitsch A, Kolenda H, et al. Inflammatory central nervous system demyelination: correlation of magnetic resonance imaging findings with lesion pathology. Ann Neurol 1997;42:783–793
5. van Walderveen MAA, Kamphorst W, Scheltens P, et al. Histopathologic correlate of hypointense lesions on T1-weighted spin-echo MRI in multiple sclerosis. Neurology 1998;50:1282–1288
6. van Walderveen MAA, Barkhof F, Pouwels PJW, et al. Neuronal damage in T1-hypointense multiple sclerosis lesions demonstrated in vivo using proton magnetic resonance spectroscopy. Ann Neurol 1999;46:79–87
7. van Waesberghe JHTM, Kamphorst W, De Groot CJA, et al. Axonal loss in multiple sclerosis lesions: magnetic resonance imaging insights into substrates of disability. Ann Neurol 1999; 46:747–754
8. Truyen L, van Waesberghe JHTM, van Walderveen MAA, et al. Accumulation of hypointense lesions ("black holes") on T_1 spin-echo MRI correlates with disease progression in multiple sclerosis. Neurology 1996;47:1469–1476
9. van Walderveen MAA, Barkhof F, Hommes OR, et al. Correlating MRI and clinical disease activity in multiple sclerosis: relevance of hypointense lesions on short-TR/short-TE (T1-weighted) spin-echo images. Neurology 1995;45:1684–1690
10. Loevner LA, Grossman RI, McGowan JC, et al. Characterization of multiple sclerosis plaques with T1-weighted MR and quantitative magnetization transfer. AJNR Am J Neuroradiol 1995;16:1473–1479
11. Grimaud J, Barker GJ, Wang L, et al. Correlation of magnetic resonance imaging parameters with clinical disability in multiple sclerosis: a preliminary study. J Neurol 1999;246:961–967
12. Rovaris M, Comi G, Rocca MA, et al. Relevance of hypointense lesions on fast fluid-attenuated inversion recovery MR images as a marker of disease severity in cases of multiple sclerosis. AJNR Am J Neuroradiol 1999;20:813–820
13. van Waesberghe JH, van Walderveen MA, Castelijns JA, et al. Patterns of lesion development in multiple sclerosis: longitudinal observations with T1-weighted spin-echo and magnetization transfer MR. AJNR Am J Neuroradiol 1998;19:675–683
14. Poser CM, Paty DW, Scheinberg L, et al. New diagnostic criteria for multiple sclerosis: guidelines for research protocols. Ann Neurol 1983;13:227–231
15. Brück W, Porada P, Poser S, et al. Monocyte/macrophage differentiation in early multiple sclerosis lesions. Ann Neurol 1995;38:788–796
16. Lassmann H, Brück W, Lucchinetti C, Rodriguez M. Remyelination in multiple sclerosis. Mult Scler 1997;3:133–136
17. Prineas JW, Barnard RO, Kwon EE, et al. Multiple sclerosis: remyelination of nascent lesions. Ann Neurol 1993;33:137–151
18. Nesbit GM, Forbes GS, Scheithauer BW, et al. Multiple sclerosis: histopathologic and MR and/or CT correlation in 37 cases at biopsy and three cases at autopsy. Radiology 1991;180: 467–474
19. van Walderveen MAA, Truyen L, van Oosten BW, et al. Development of hypointense lesions on T_1-weighted spin-echo magnetic resonance images in multiple sclerosis. Relation to inflammatory activity. Arch Neurol 1999;56:345–351
20. Simon JH, Lull J, Jacobs LD, et al. A longitudinal study of T1 hypointense lesions in relapsing MS. MSCRG trial of interferon β-1a. Neurology 2000;55:185–192

A SURF1 Gene Mutation Presenting as Isolated Leukodystrophy

Shamina Rahman, MRCP,[1] Ruth M Brown, MSc,[3] Wui Khean Chong, FRCR,[2] Callum J Wilson, FRACP,[1] and Garry K Brown, FRCP, PhD[3]

Mitochondrial respiratory chain defects are increasingly recognized in patients with leukodystrophy. We report the first case of leukodystrophy with systemic cytochrome oxidase deficiency caused by a loss of function mutation in the SURF1 gene in a 2-year-old girl presenting with failure to thrive, global neurodevelopmental regression, and lactic acidosis. Although all previously reported mutations in the SURF1 gene have been found in patients with cytochrome oxidase (COX)-deficient Leigh syndrome, the phenotype associated with SURF1 protein deficiency should be extended to include leukodystrophy.

Ann Neurol 2001;49:797–800

The inherited leukodystrophies comprise a heterogeneous group of neurodegenerative disorders principally affecting the white matter of the brain.[1] Clinical features are extremely variable, but motor manifestations usually predominate. A period of normal development usually precedes onset of neurological symptoms and signs and loss of skills. Seizures are rare and cognitive deterioration usually occurs late in the clinical course. Characteristically neuroimaging demonstrates bilateral symmetrical signal abnormality in the white matter. Current biochemical classifications are incomplete as the underlying metabolic defect is unknown in many cases.

The isolated finding of diffuse leukodystrophy is a rare but increasingly recognized manifestation of mitochondrial respiratory chain defects.[2–6] Among the respiratory chain deficiencies presenting in infancy and early childhood, cytochrome oxidase (COX) deficiency is the most commonly diagnosed.[7] At present, it appears that mutations in the SURF1 gene, which encodes a protein involved in COX assembly, are responsible in a significant proportion of patients.[8,9] All patients previously reported with SURF1 mutations have had Leigh syndrome, a neurodegenerative disorder with characteristic basal ganglia and brainstem lesions. Although white matter lesions may be observed in Leigh syndrome, they are not a major neuropathological feature of this disorder. We now report a homozygous mutation in the SURF1 gene in a child with isolated leukodystrophy.

From the Departments of [1]Metabolic Medicine and [2]Radiology, Great Ormond Street Hospital, London; and [3]Genetics Unit, Department of Biochemistry, University of Oxford, UK

Received Dec 26, 2000 and in revised form Mar 15, 2001. Accepted for publication Mar 15, 2001.

Address correspondence to Dr Rahman, Biochemistry, Endocrinology, and Metabolism Unit, Institute of Child Health, 30 Guilford Street, London, WC1N 1EH, UK. E-mail: S.Rahman@ich.ucl.ac.uk

Patient Details

A two-year-old girl was referred for investigation of failure to thrive associated with metabolic acidosis. The second daughter of healthy consanguineous Bengali parents, she was born after a normal pregnancy by vaginal delivery. There were no neonatal problems, but poor growth was noted from 9 months. At 11 months she had an episode of cyanosis and floppiness, without preceding intercurrent illness, and subsequently her developmental milestones slowed. At 1 year of age she was able to pull to stand, cruise around furniture, and crawl. An older sister is well and there is no family history of neurological disease. Examination at 2 years revealed weight, height, and head circumference all below the third centile. There were no dysmorphic features. She had mild hypotonia with normal deep tendon reflexes. Initial investigations revealed lactic acidosis with plasma lactate between 3.2 and 5.7 mmol/l (normal <1.8) and lactate/pyruvate ratios between 22 and 26 (normal <20).

Magnetic resonance imaging (MRI) of the brain performed at 2 years and 5 months demonstrated abnormal signal in the cerebral white matter, particularly posteriorly, with signal change in the posterior limbs of the internal capsule, corpus callosum (particularly the splenium), dentate nuclei, and adjacent cerebellar white matter (Fig 1A, 1B). Areas within the more confluent white matter abnormalities appeared to be cystlike (Fig 1C, 1D). No abnormalities were seen in the caudate or lentiform nuclei. There were small bilateral slightly asymmetric lesions in the medulla, predominantly involving the olives and inferior cerebral peduncles. With the predominant abnormalities being in the white matter, the appearances were considered to be those of leukoencephalopathy with involvement of the corticospinal tracts. Electroencephalogram revealed mild nonspecific abnormality, with excess fast activity over the anterior half of the head and rhythmic intermediate slow activity posteriorly. There were no vacuolated lymphocytes in the blood film and activities of leukocyte lysosomal enzymes were all within the normal range. Plasma very long chain fatty acid levels were also normal, and transferrin isoelectric focusing showed a normal pattern.

At 2 years 8 months, she had lost skills. She had fewer words and less clear speech. Her floppiness had

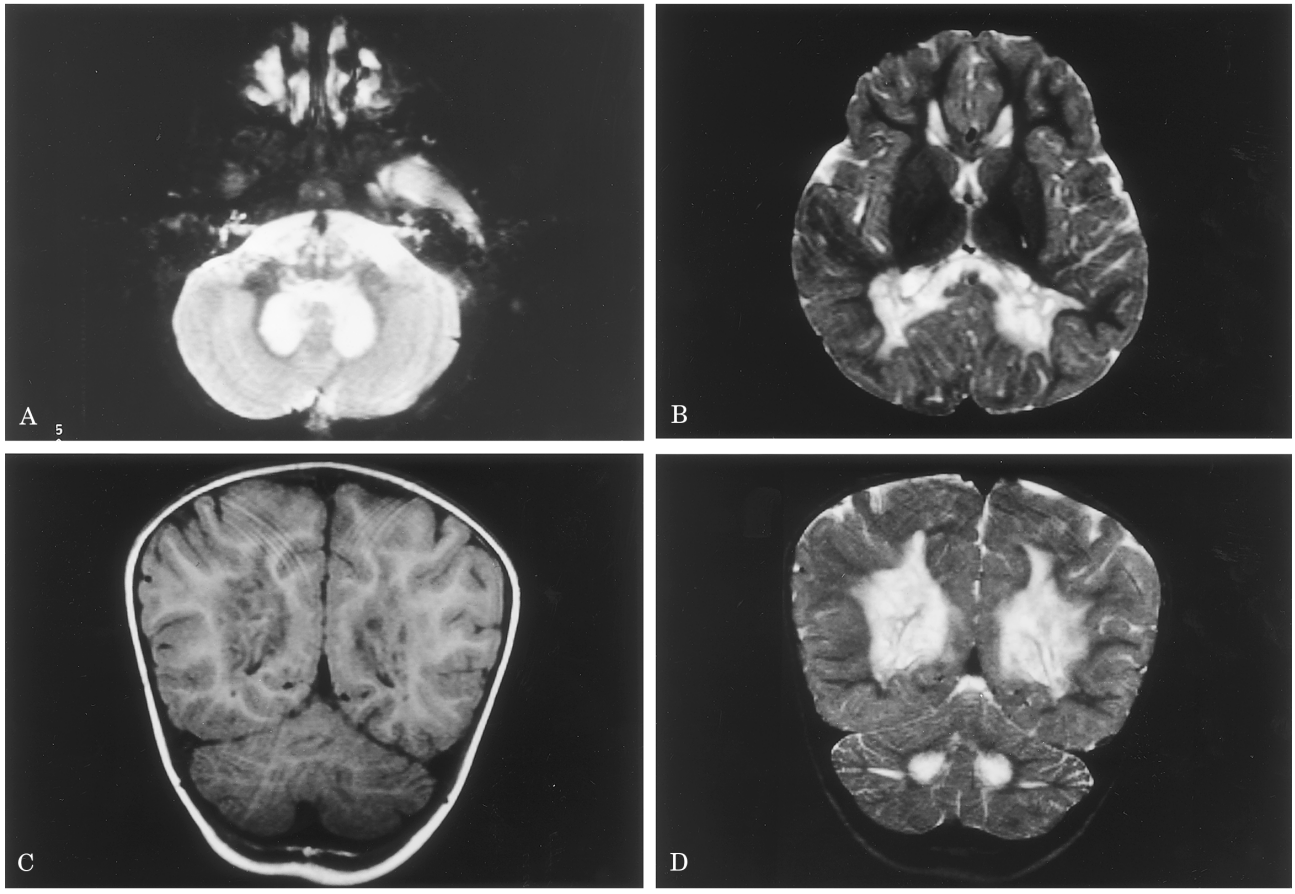

Fig 1. Magnetic resonance images of the patient's brain at age 2 years 5 months. (A) Axial T2-weighted image demonstrating abnormal high signal in the cerebellar white matter. (B) Axial T2-weighted image demonstrating abnormal high signal in the splenium and internal capsule. No lesions are visible in the basal ganglia. (C) Coronal T1-weighted image demonstrating cystlike lesions in the white matter. (D) Cystlike lesions in the white matter are also seen in this coronal T2-weighted image, which also demonstrates abnormal high signal in the cerebral and cerebellar white matter.

progressed and she was barely able to sit without support. She had generalized symmetrical hypotonia and pathologically brisk reflexes with upgoing plantar responses. She continued to fail to thrive and was tachypnoeic. She was hirsute. She had poor to moderate visual acuity; eye movements were full with intermittent beats of nystagmus, and there was no evidence of optic atrophy or pigmentary retinopathy. Neurophysiological studies demonstrated normal electroretinogram but marked postretinal dysfunction on visual evoked potentials.

Paired blood and CSF lactates were 6.8 and 7.65 mmol/l respectively (normal for CSF <2). CSF protein was mildly elevated at 0.58 g/l (reference range 0–0.3). Further investigations revealed slightly abnormal renal tubular function with a mildly elevated urinary N-acetylglucosaminidase/creatinine ratio of 83 units/mmol (reference range 3.5–27.3), normal liver function, and normal echocardiogram with no evidence of cardiomyopathy.

Histology of an open quadriceps muscle biopsy showed only a mild increase in cytoplasmic fat and atrophy of Type II fibers. No ragged red fibers were seen. Respiratory chain enzyme assays on the biopsied muscle revealed a severe isolated deficiency of COX (COX/CS ratio 0.004, reference range 0.014–0.034) with normal activities of complexes I (0.113, reference range 0.104–0.268) and II/III (0.049, reference range 0.040–0.204). Severe COX deficiency was also expressed in cultured skin fibroblasts with activity <1 nmole/mg protein/min compared with a normal range of 30 to 90.

Methods

Messenger RNA was isolated from cultured skin fibroblasts using the High Pure RNA isolation kit (Boehringer Mannheim) and cDNA was synthesized using the Omniscript RT kit (Qiagen). SURF1 cDNA was amplified using oligonucleotide primers 5′-AGGAGCGTCCTCAGGGTC-3′ (forward) and 5′-CATGATCCAGCATAAAGGCA-3′ (reverse). The amplified fragment covers all of the SURF1 coding region apart from exon 1 and the first part of exon 2.

Genomic DNA was extracted from cultured skin fibroblasts using the Nucleon BACC2 kit (Nucleon) and a DNA fragment encompassing exons 6 to 9 was amplified using oligonucleotide primers 5′-TGCCTGAGTGACCATGAGTG-3′ (forward) and 5′-TGGGAAAGTTCTTTGGACTGA-3′ (reverse). Sequence analysis was performed in an automated ABI 377 sequencer using the cDNA PCR primers and Big Dye™ Terminator Cycle Sequencing kit (Applied Biosystems). The mutation in exon 8 was confirmed by restriction endonuclease digestion of the exons 6 to 9 genomic fragment with *BsrI* as the mutation creates an additional restriction site for this enzyme.

Results

Sequence analysis of the coding region of the SURF1 gene of the patient revealed only a single sequence in which there was a 2-bp deletion in exon 8. The deletion involves one of a pair of AG dinucleotides after nucleotide 789 (numbering from the ATG start codon), and as it is not possible to determine which pair is deleted, the mutation has been arbitrarily designated del AG 790–791. This mutation would lead to a frameshift after threonine 263 and the generation of a new stop codon after a further 26 amino acids. Restriction endonuclease analysis of genomic DNA with BsrI demonstrated that the patient was homozygous for this mutation and that both parents were heterozygous (Fig 2).

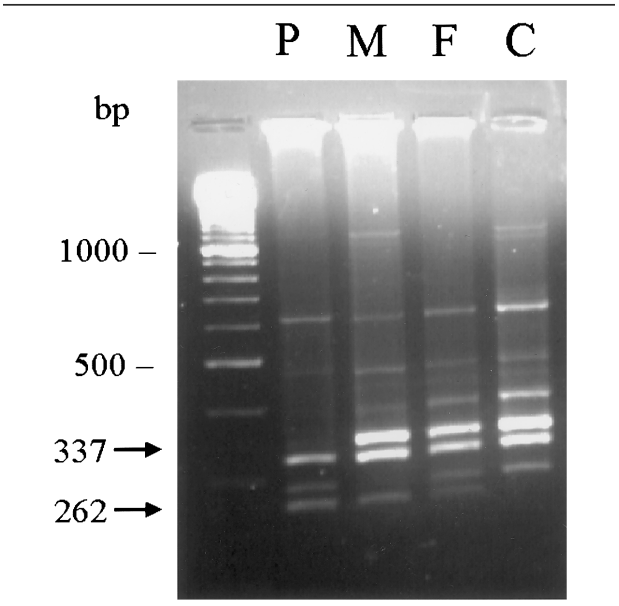

Fig 2. Demonstration of the SURF1 mutation in genomic DNA. A segment of the SURF1 gene encompassing exons 6 to 9 and digested with the restriction enzyme BsrI is shown. The AG deletion in exon 8 leads to formation of a new BsrI site with the result that the 337-bp restriction fragment is further digested into 262 and 75 bp fragments. The patient (P) is homozygous for this deletion, while both parents (M and F) are heterozygous. A normal control (C) is shown for comparison. The left-hand track is a 100 bp molecular size ladder with the 500 and 1,000 bp fragments indicated.

Discussion

We report a patient with a mutation in the SURF1 gene, predicted to produce a truncated protein and complete deficiency of SURF1 protein. The patient had significant neurological dysfunction associated with extensive white matter changes in the cerebrum and cerebellum. Multiple, small, cystlike white matter lesions, similar to those described in 2 of 5 families previously reported with leukodystrophy and respiratory chain defects, were observed within the more confluent white matter abnormalities.[10] It is possible that these cystlike lesions may be a specific feature of white matter disease caused by respiratory chain defects.

All patients with SURF1 mutations previously reported have had Leigh syndrome and COX deficiency, leading to the suggestion that loss of function mutations of SURF1 are exclusively associated with this phenotype.[11] We now demonstrate that SURF1 mutations may be associated with more than one neuroradiological pattern, ie, diffuse leukodystrophy as well as Leigh syndrome. Levels of residual COX activity in skeletal muscle and cultured skin fibroblasts in our patient were similar to those in patients with SURF1 mutations and Leigh syndrome.[11] Of particular note is a report of typical Leigh syndrome in a patient heterozygous for the same AG deletion in exon 8 as our patient. In the previous patient, the mutation in the second SURF1 gene resulted in substitution of aspartic acid for tyrosine 274.[12] By contrast, the patient we describe had no evidence of the basal ganglia necrotic lesions that are characteristic of Leigh syndrome. The reason for the different pattern of neuropathology in these 2 patients is unclear, but it is possible that it is related to the presence of two different SURF1 mutations in the previously reported case. However phenotypic heterogeneity associated with identical mutations has previously been described in other single gene disorders.[13]

The search for SURF1 mutations has focused mainly on patients with Leigh syndrome or with "Leigh-like" features. The identification of a pathogenic SURF1 mutation in a patient with isolated leukodystrophy leads us to suggest that mitochondrial respiratory chain enzymes should be assayed in patients with leukodystrophy and lactic acidosis, and the SURF1 gene sequenced in those with isolated COX deficiency. Furthermore, the SURF1 gene should be analyzed in all patients with isolated COX deficiency, to determine the range of phenotypes that may be associated with mutations in this gene.

References

1. Aicardi J. The inherited leukodystrophies: a clinical overview. J Inherit Metab Dis 1993;16:733–743.

2. Loeffen JL, Smeitink JA, Trijbels JM, et al. Isolated complex I deficiency in children: clinical, biochemical and genetic aspects. Hum Mutat 2000;15:123–134.
3. Pined JM, Marsac C, Barkaoui E, et al. Leigh syndrome and leukodystrophy due to partial succinate dehydrogenase deficiency: regression with riboflavin. Arch Pediatr 1999;6:421–426.
4. Schuelke M, Smeitink J, Mariman E, et al. Mutant NDUFV1 subunit of mitochondrial complex I causes leukodystrophy and myoclonic epilepsy. Nat Genet 1999;21:260–261.
5. Harpey JP, Heron D, Prudent M, et al. Diffuse leukodystrophy in an infant with cytochrome-c oxidase deficiency. J Inherit Metab Dis 1998;21:748–752.
6. Rabano JA, Playan A, Guirado F, et al. Acute presentation of leukodystrophy due to mitochondrial cytopathology and multiple deletions of mitochondrial DNA. Rev Neurol 1998;27: 1005–1007.
7. Jaksch M, Hofmann S, Kleinle S, et al. A systematic mutation screen of 10 nuclear and 25 mitochondrial candidate genes in 21 patients with cytochrome c oxidase (COX) deficiency shows tRNA(Ser)(UCN) mutations in a subgroup with syndromal encephalopathy. J Med Genet 1998;35:895–900.
8. Tiranti V, Hoertnagel K, Carrozzo R, et al. Mutations of SURF-1 in Leigh disease associated with cytochrome c oxidase deficiency. Am J Hum Genet 1998;63:1609–1621.
9. Zhu Z, Yao J, Johns T, et al. SURF1, encoding a factor involved in the biogenesis of cytochrome c oxidase, is mutated in Leigh syndrome Nat Genet 1998;20:337–343.
10. de Lonlay-Debeney P, von Kleist-Retzow JC, Hertz-Pannier L, et al. Cerebral white matter disease in children may be caused by mitochondrial respiratory chain deficiency. J Pediatr 2000; 136:209–214.
11. Tiranti V, Jaksch M, Hofmann S, et al. Loss-of-function mutations of SURF-1 are specifically associated with Leigh syndrome with cytochrome c oxidase deficiency. Ann Neurol 1999;46:161–166.
12. Teraoka M, Yokoyama Y, Ninomiya S, et al. Two novel mutations of SURF1 in Leigh syndrome with cytochrome c oxidase deficiency. Hum Genet 1999;105:560–563.
13. Wolf U. Identical mutations and phenotypic variation. Hum Genet 1997;100:305–321.

Slowing of Voluntary and Involuntary Saccades: An Early Sign in Spinocerebellar Ataxia Type 7

Andrew K. Oh, MD,[1] Kathleen M. Jacobson,[1]
Joanna C. Jen, MD, PhD,[1] and Robert W. Baloh, MD[1,2]

We describe quantitative oculomotor findings in a patient with subclinical spinocerebellar ataxia type 7 (SCA7) and a borderline mutation of 38 CAG repeats and her daughter with SCA7 and 46 repeats. Both subjects demonstrated significant slowing of voluntary and involuntary saccades, but retinal examination was normal. Smooth pursuit and fixation suppression of VOR were mildly impaired. Slow saccades may be the earliest neurologic finding even in asymptomatic SCA7 patients with normal ocular fundi. The SCA7 mutation probably has an early impact on brainstem fast eye movement centers.

Ann Neurol 2001;49:801–804

SCA7 belongs to a heterogeneous group of autosomal dominant cerebellar ataxias in which the disease-causing mutation is an expansion of an unstable CAG trinucleotide repeat, resulting in a polyglutamine-expanded protein.[1] Within this group of ataxias, which also includes SCA1, SCA2, SCA3, and SCA6, the clinical features overlap to such an extent that distinction between the different SCAs is often difficult. The presence of pigmentary macular dystrophy distinguishes SCA7. Normal repeat size in the SCA7 gene is up to 17, whereas mutant alleles have 38 or more.[1] Using quantitative eye movement analysis, distinct oculomotor patterns were recently identified in SCA1, SCA2, SCA3, and SCA6, shedding light on the differential localization of neuropathology in the different SCAs.[2] Until now, the oculomotor signs in SCA7 have not been well documented using quantitative methods.

From the Departments of [1]Neurology and [2]Surgery (Head and Neck), University of California Los Angeles School of Medicine, Los Angeles, CA

Received Dec 11, 2000 and in revised form Mar 1, 2001 and Mar 14, 2001. Accepted for publication Mar 15, 2001.

Address correspondence to Dr Baloh, Department of Neurology, UCLA School of Medicine, 710 Westwood Plaza, Box 951769, Los Angeles, CA 90095-1769. E-mail: rwbaloh@ucla.edu

Methods

Patients

We studied an SCA7 family in which an intergenerational CAG repeat expansion occurred between a normal mother and her affected daughters (Fig 1). The proband was a 34-year-old woman who presented with a 4-year history of ataxia, incoordination, dysarthria, and diplopia. She denied a family history of similar problems. Visual acuity was normal, but by the time of a 2-year follow-up examination, visual acuity without correction was 20/100 (+2) OD and 20/80 (-2) OS, with no improvement with pinhole. Quantitative visual field testing and fluorescein angiography were normal. Bedside examination showed slowing of both vertical and horizontal saccades, a wide-based ataxic gait, limb dysmetria, dysdiadochokinesia, cerebellar dysarthria, generalized spasticity with hyperreflexia, and sustained ankle clonus bilaterally. Funduscopic examination was normal (see Fig 1). Brain MRI documented cerebellar and pontine atrophy that was significant for her age (see Fig 1). SCA7 mutation analysis (Baylor DNA Diagnostic Laboratory, Houston, TX) detected an allele with 46 repeats. The proband's brother was 2 years older and had noted gait imbalance for 3 years, but he died of unrelated causes before he could be examined. The proband's 38-year-old sister, who noted mild imbalance but no visual loss, had 42 repeats but was unavailable for examination or oculomotor testing. The proband's 66-year-old mother reported no gait imbalance and no visual loss. She had normal visual acuity with correction. Funduscopic examination showed macular drusen but was within normal limits (see Fig 1). Bedside visual field testing was normal. She had mild difficulty with tandem gait that was within the range of normal for her age. She could take three to four steps in tandem before taking a side step. Both vertical and horizontal saccades appeared normal to clinical examination. Brain MRI revealed mild cerebellar and pontine atrophy (see Fig 1). She had a mutant allele with 38 repeats, the smallest number considered a mutation.[1] Both neurologic examination and SCA7 genetic testing of the father were normal.

Eye Movement Recordings and Data Analysis

Informed consent was obtained from all subjects. Direct-current electro-oculographic recordings were performed to measure saccades, smooth pursuit, and spontaneous and gaze-evoked nystagmus, rotation-induced nystagmus (VOR), and fixation suppression of VOR (VOR-fix). Our method of eye movement recordings and online computer data analysis has been described in detail previously.[3,4]

Results

The quantitative oculomotor findings in our patients are summarized in the Table. Voluntary saccadic peak velocity was profoundly depressed in the proband (Fig 2A, C). Her asymptomatic mother also showed significant slowing of saccades. Saccades had prolonged latency but normal accuracy in both subjects. Upbeat nystagmus was seen on upgaze in the proband. Smooth pursuit in both subjects was normal at low velocities. At higher velocities, pursuit gain was significantly below normal (see Table). Mild impairment of fixation

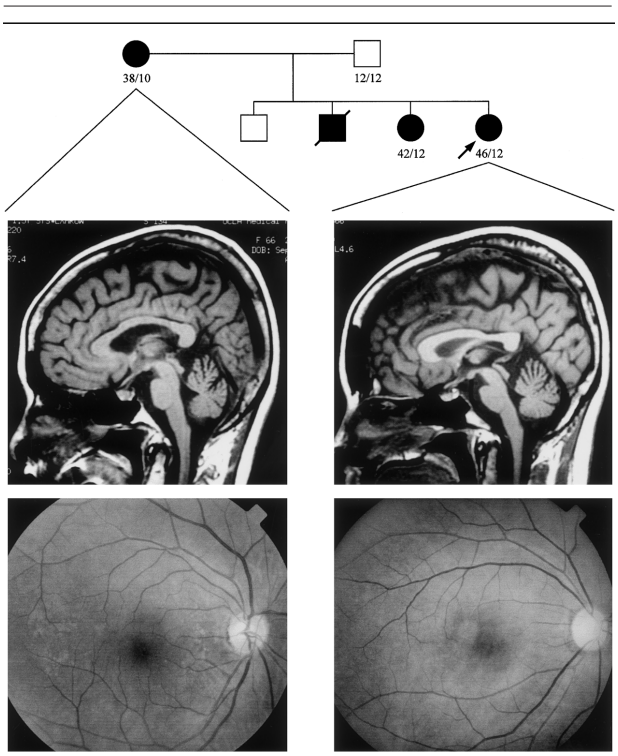

Fig 1. SCA7 family pedigree. ■ ● = *affected individuals.* □ ○ = *unaffected individuals.* ↑ = *proband. CAG repeat number is indicated for each allele where known. Upper panels: Sagittal T1-weighted brain MRI showing mild and moderate pontine atropy in the mother and proband, respectively. Lower panels: Ocular fundi (right eye shown) were normal bilaterally in each subject.*

suppression of the VOR, consistent with the smooth pursuit deficit, met statistical significance compared to normal controls. Rotation-induced nystagmus was abnormal, caused either by slowing or impaired triggering of involuntary saccades, or a combination of these factors. This affected our ability to assess VOR at low frequencies of sinusoidal rotation (see Fig 2B). However, VOR gain was normal at higher-frequency rotations that did not require corrective fast components (see Table). Overall, abnormalities of the fast eye movement system were the predominant finding in both subjects. We subsequently tested a third, unrelated SCA7 patient and found an identical pattern of oculomotor abnormalities, suggesting that slowing of saccades is a common finding in SCA7 (data not shown).

Discussion

Comparison with Previous Studies and Clinicopathologic Correlation

Slowing of saccades on clinical examination of SCA7 patients has been mentioned previously. Gouw and colleagues noted slowing of saccades in a large kindred with autosomal- dominant cerebellar ataxia and retinal degeneration.[5] Genetic classification of these individuals later confirmed mutations in the SCA7 gene.[6] Our quantitative data confirm these clinical findings and show that impaired fast eye movements were an early sign of disease in an asymptomatic carrier with a normal bedside examination including normal ocular fundi.

By virtue of the severe slowing of voluntary and involuntary saccades, our patients had a combination of oculomotor findings that most closely resembles SCA2.[2] Buttner and colleagues reported that all of their SCA2 patients had a profound reduction of saccade peak velocity.[2] SCA1 patients also had saccade slowing but to a lesser degree. Analogous to our cases with SCA7, very early slowing of saccades has been reported in patients with SCA2.[7] Together, these find-

Table. Quantitative Oculomotor Findings in SCA7 Patients (Mean ± 1 Standard Deviation)

	Saccades[a]		Pursuit Gain[b]		VOR Gain[c]		VOR-Fix[c]
	PV (degrees/second)	Latency (seconds)	0.2 Hz (24 degrees/second)	0.4 Hz (47 degrees/second)	0.05 Hz (60 degrees/second)	0.8 Hz (30 degrees/second)	0.05 Hz (60 degrees/second)
Proband	204 ± 14[d]	270 ± 22[d]	0.90 ± 0.03	0.50 ± 0.04[d]	ifc	0.85 ± 0.20	0.08 ± 0.02[d]
Mother	317 ± 41[d]	426 ± 26[d]	0.85 ± 0.07	0.53 ± 0.04[d]	ifc	0.80 ± 0.13	0.13 ± 0.02[d]
Normal[3,4]	486 ± 60	176 ± 18	0.92 ± 0.08	0.87 ± 0.11	0.50 ± 0.15	0.72 ± 0.11	0.03 ± 0.02

[a]Stimulus consisted of a pseudorandomized sequence of target steps between 6 and 36 degrees of horizontal amplitude in both directions (total of 42 steps). Average peak velocity shown is for saccades that fell within bins of 30 ± 2 degrees amplitude. Each bin contained an average of 7 and a minimum of 4 saccades. Abducting and adducting saccades of the right eye were averaged. Latency shown is an average of saccade reaction time for all 42 saccades.
[b]Smooth pursuit was triggered by a sinusoidal target moving constantly between ± 18 degrees of amplitude.
[c]Subjects sat with eyes open in darkness in a rotatory chair with a fixation light turned off (VOR) or, during separate trials, with a fixation light turned on (VOR-fix).
[d]$p < .01$, one-tailed t test assuming unequal variance.

PV = average peak velocity; VOR = vestibulo-ocular reflex; VOR-fix = fixation suppression of VOR; ifc = impaired fast components (see Fig 2B).

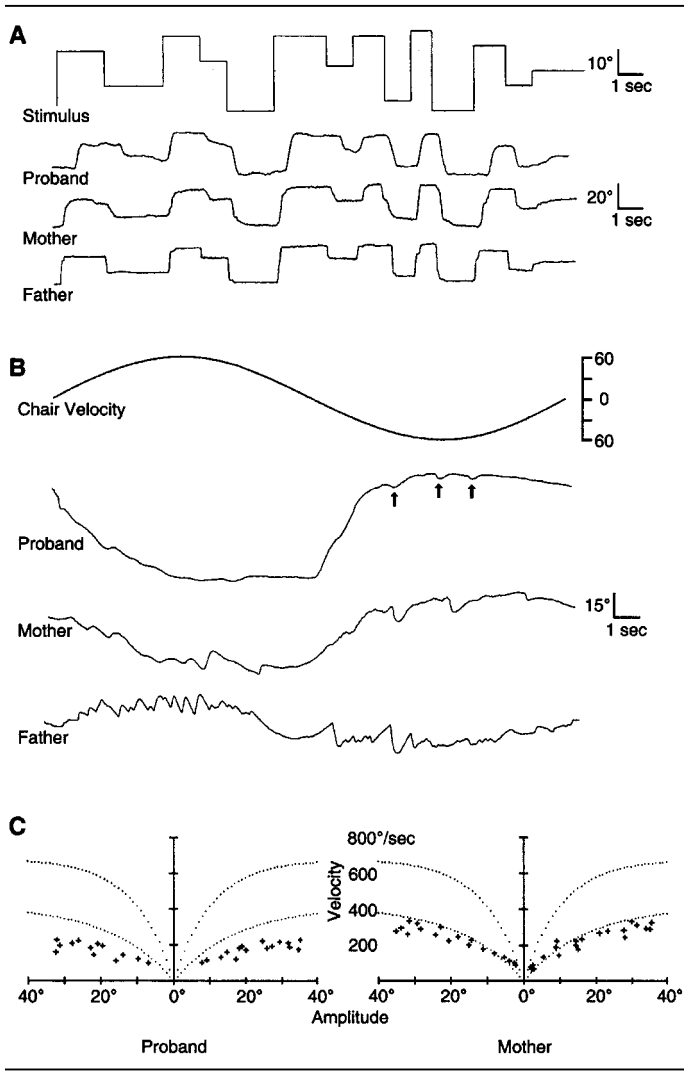

Fig 2. Horizontal monocular electro-oculographic recordings of saccadic (A) and vestibular (B) eye movements in the proband and her mother. The father's recordings are shown as a normal control. (A) Slowing of voluntary saccades is most prominent in the proband and found to a lesser degree in the mother. (B) Sinusoidal (0.05 Hz, 60°/second peak velocity) rotation in the dark showing impaired production of fast components in the proband and mother. Note that the eyes deviate in the direction of the fast components in the normal father but deviate in the direction of the slow components in the proband and mother, which may be caused by slow inadequate fast components (arrows) *and a defect in triggering fast components. (C) Plots of horizontal voluntary saccade peak velocity vs amplitude (right eye shown) in the proband and her mother. Though the mother's saccades did not appear slow to clinical bedside examination, they were significantly below normal velocity on quantitative testing. Dotted lines represent normal mean ± two standard deviations.*

ings suggest that brainstem regions that mediate the generation of saccadic eye movements are an early site of neurodegeneration in both SCA2 and SCA7. The fact that the mother in our study had significant slowing of horizontal saccades without visual loss or ataxia suggests that loss of excitatory burst neurons (EBN) in the paramedian pontine reticular formation (PPRF) may precede clinically significant loss of retinal and cerebellar Purkinje cells (PC). Patients with SCA2 and SCA7 both show pontine atrophy.[5,8] Moreover, Horn and colleagues reported that postmortem examination of a patient with SCA2 demonstrated specific loss of EBN responsible for horizontal saccades in the nucleus reticularis pontis caudalis.[9] We are not aware of any similar studies of the brains of SCA7 patients, but we would anticipate a similar neuropathologic pattern on the basis of our current oculomotor findings.

Implications of Current Findings on SCA7 Neuropathogenesis

The exact manner in which the SCA7 gene product ataxin-7, when carrying an abnormal polyglutamine expansion, might yield selective degeneration of a specific neuronal population is not known. In three other CAG

trinucleotide repeat diseases—SCA1, SCA3, and Huntington's disease—it has been demonstrated that neuronal intranuclear inclusions (NII) composed of the corresponding polyglutamine proteins develop chiefly in neuronal populations that are affected by the disease.[10] Ataxin-7-containing NII have been described in a patient with SCA7, but these inclusions were not restricted to brain regions affected by severe neuronal loss.[10]

Recent studies of mutant and wild-type ataxins provide potential explanations for the selective loss of EBN early in the course of SCA7. Mutant ataxin-7 may interact in a deleterious way with other cell type-specific proteins found only in the neuronal populations at risk. EBN in the PPRF are known to express high levels of the calcium-binding protein parvalbumin.[9] In fact, parvalbumin immunoreactivity was exploited in the original histologic identification of EBN in humans.[9] Parvalbumin is also highly expressed in PC.[11] Experiments with a transgenic mouse model of SCA1 have demonstrated that early in the course of disease there is reduced PC expression of calcium-binding proteins calbindin-D28k and parvalbumin.[11] This decreased expression was shown to occur prior to the appearance of NII. The expression of parvalbumin and calbindin is thought to be highest in neuronal populations that have fast firing rates and that have relatively high oxidative metabolism,[9] including EBN and PC. One potential mechanism of SCA7 neurodegeneration would therefore involve diminished expression of proteins responsible for critical calcium-related functions such as calcium buffering or other calcium-mediated processes.

In addition to potential effects of mutant ataxin-7, a greater understanding of the normal function of this protein may yield further insight into SCA7 neuropathogenesis. Taken as a whole, ataxin-7 shares no homology with known proteins and its exact function is unknown. However, ataxin-7 was recently found to share a relatively small phosphoprotein-binding motif with arrestins, proteins that bind to and inactivate phosphorylated-activated forms of several G-protein-coupled receptors, including rhodopsin and the beta-adrenergic receptor.[12] Arrestin binding is thereby critical in preventing prolonged signal transduction. The presence of an arrestin-like binding site suggests that one function of ataxin-7 is to inactivate another protein that might otherwise remain constitutively activated. If this is the case, the results of our study suggest that the next step in understanding the topography of neurodegeneration in SCA7 might be to identify an ataxin-7-binding phosphoprotein that is selectively expressed in rapidly firing cells such as pontine EBN.

Normal VOR in SCA7

Though brainstem centers for saccade generation appear to be markedly affected in SCA7, VOR was normal. At first glance, VOR appeared to be impaired in both of our subjects at low frequencies of sinusoidal rotation. However, rotation-induced nystagmus was poorly formed in these subjects. This was the result of both slowing and impaired triggering of the fast components of nystagmus (see Fig 2B). Fast components were so impaired that at high-amplitude, low-frequency rotations, the subjects' eyes deviated slowly and became pinned at the point of maximal excursion within the orbit. However, VOR was normal at higher frequencies and lower amplitudes that do not require corrective fast components (see Table).

Supported by grants P01 DC02952 and T32 DC00008-23 from the National Institutes of Health.

References

1. David G, Abbas N, Stevanin G, et al. Cloning of the SCA7 gene reveals a highly unstable CAG repeat expansion. Nat Genet 1997;17:65–70.
2. Buttner N, Geschwind D, Jen JC, et al. Oculomotor phenotypes in autosomal dominant ataxias. Arch Neurol 1998;55: 1353–1357.
3. Baloh RW, Honrubia V. Clinical neurophysiology of the vestibular system. Philadelphia: Davis, 1990.
4. Moschner C, Baloh RW. Age-related changes in visual tracking. J Gerontol 1994;49:M235–M238.
5. Gouw LG, Digre KB, Harris CP, et al. Autosomal dominant cerebellar ataxia with retinal degeneration: clinical, neuropathologic, and genetic analysis of a large kindred. Neurology 1994; 44:1441–1447.
6. Gouw LG, Castaneda MA, McKenna CK, et al. Analysis of the dynamic mutation in the SCA7 gene shows marked parental effects on CAG repeat transmission. Hum Mol Genet 1998;7: 525–532.
7. Wadia N, Pang J, Desai J, et al. A clinicogenetic analysis of six Indian spinocerebellar ataxia (SCA2) pedigrees: the significance of slow saccades in diagnosis. Brain 1998;121:2341–2355.
8. Burk K, Abele M, Fetter M, et al. Autosomal dominant cerebellar ataxia type I: clinical features and MRI in families with SCA1, SCA2 and SCA3. Brain 1996;119:1497–1505.
9. Horn AKE, Buttner-Ennever JA, Buttner U. Saccadic premotor neurons in the brainstem: functional neuroanatomy and clinical implications. Neuro-ophthalmology 1996;16:229–240.
10. Holmberg M, Duyckaerts C, Durr A, et al. Spinocerebellar ataxia type 7 (SCA7): a neurodegenerative disorder with neuronal intranuclear inclusions. Hum Mol Genet 1998;7:913–918.
11. Vig PJS, Subramony SH, Qin Z, et al. Relationship between ataxin-1 nuclear inclusions and Purkinje cell specific proteins in SCA-1 transgenic mice. J Neurol Sci 2000;174:100–110.
12. Mushegian AR, Vishnivetskiy SA, Gurevich VV. Conserved phosphoprotein interaction motif is functionally interchangeable between ataxin-7 and arrestins. Biochemistry 2000;39: 6809–6813.

Intermediate CAG Repeat Lengths (53,54) for MJD/SCA3 Are Associated with an Abnormal Phenotype

Nens van Alfen, MD,[1] Richard J. Sinke, PhD,[1,4]
Michael J. Zwarts, MD, PhD,[2]
Anneke Gabreëls-Festen, MD, PhD,[3]
Peter Praamstra, MD, PhD,[1]
Berry P.H. Kremer, MD, PhD,[1]
Martin W.I.M. Horstink, MD, PhD[1]

We report on a Dutch family in which 4 members in 2 generations have intermediate repeat lengths (53 and 54) for Machado-Joseph Disease/ Spinocerebellar Ataxia (MJD/SCA3). All but the youngest have a restless legs syndrome with fasciculations and a sensorimotor axonal polyneuropathy. Central neurological abnormalities are only present in 2. This family shows that intermediate repeat lengths can be pathogenic and may predispose for restless legs and peripheral nerve disorder.

Ann Neurol 2001;49:805–808

Machado-Joseph disease (MJD), also called spinocerebellar ataxia type 3 (SCA3), is an autosomal dominantly inherited progressive neurodegenerative disorder caused by CAG trinucleotide repeat expansions in the MJD/SCA3 gene. Normal alleles contain 12 to 44 repeats, whereas in MJD/SCA3 patients the number of repeats of the affected allele usually varies between 60 and more than 85.[1,2] The neurodegenerative process in MJD/SCA3 is influenced by the size of the expanded CAG repeat, which correlates with the age of onset, clinical expression, and progression of the disease.[3] Four clinical subtypes are usually distinguished.[4,5] Type I tends to have the longest repeats, the earliest onset (15–30 years), and the most rapid progression with marked pyramidal and extrapyramidal signs in addition to the common features of ataxia and ophthalmoplegia. The age at onset of the most common Type II is usually between 20 and 45 years; the features are limited to cerebellar and pyramidal signs. Type III shows later onset (40–60 years) and a slow progression of cerebellar signs and peripheral neuropathy. The rare Type IV is characterized by the latest onset (>50 years) with parkinsonism and polyneuropathy. In contrast to other CAG repeat expansion disorders such as Huntington's disease, there appears to be a gap in the repeat lengths of normal and affected alleles. Only two patients with intermediate alleles (n = 54 and 56) have been reported,[6,7] and there are no reports of intermediate repeats in healthy subjects. Hence, the phenotype of such intermediate MJD/SCA3 alleles remains uncertain.

There is an association between MJD/SCA3 and the restless legs syndrome (RLS), which is reported as a frequent cause of sleep disturbance in MJD.[8] We report a family in which four members have intermediate MJD/SCA3 alleles (see Figure); all but the youngest have RLS, a sensorimotor axonal polyneuropathy, and fasciculations. Two members have central neurological signs (see Table).

Patients

The proband (II-2) is a 66-year-old man who has suffered from the age of 53 from trembling hands and legs, unsteady gait, and calf cramps. Two years later he showed slight mask facies, moderate resting and postural tremor in the arms and postural tremor in the trunk, head and upper legs, slight rigidity, low tendon reflexes, bilateral extensor toe responses, bilateral peroneal palsy, and decreased vibration sense at the ankles. Distal muscle atrophy in legs and arms and generalized fasciculations are also present. Currently, the main problem is a locomotor disability requiring a walking stick (tandem gait is impossible) and a positive Romberg's test. Proximal muscular atrophy has resulted in an inability to stand up without using his hands. Levodopa therapy has a beneficial effect on tremor. Levodopa dyskinesias remain absent, despite more than 10 years of therapy. From the beginning, the patient fulfilled the minimal diagnostic criteria of RLS necessary for diagnosis;[9] i.e., (1) desire to move the limbs associated with unpleasant sensations in the legs, (2) motor restlessness relieving the discomfort in the limbs, (3) symptoms worsen at rest, and (4) symptoms worsen in evening or night. Levodopa suppressed RLS. Magnetic resonance imaging (MRI) and ^{123}I-iodobenzamide (I-IBZM) single photon emission tomography (SPECT) were normal. EMG (see Table) showed moderately lowered motor and sensory responses distally. The H-reflex was delayed. Needle EMG revealed chronic neurogenic changes in distal leg muscles (see Table). A 5-Hz resting tremor was also seen with simultaneous agonist and antagonist activity. Nerve conduction studies disclosed only slightly abnormal motor

From the Departments of [1]Neurology, [2]Clinical Neurophysiology, and [3]Neuromorphology, University Medical Center, Nijmegen, and [4]Department of Medical Genetics, University Medical Center, Utrecht, The Netherlands

Received Apr 20, 2000 and in revised form Feb 20, 2001. Accepted for publication Feb 20, 2001.

Address correspondence to Dr Horstink, Department of Neurology, University Medical Center, PO Box 9101, 6500 HB Nijmegen, The Netherlands. E-mail: M.Horstink@czzoneu.azn.nl

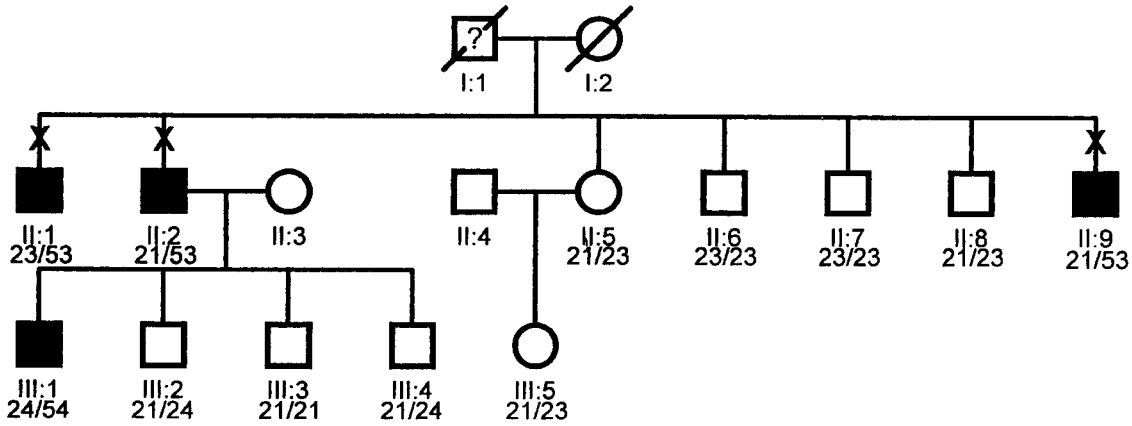

Fig. Pedigree showing the repeat length of all persons who underwent clinical examination and DNA analysis. Filled symbols = *persons with intermediate repeat length. X = persons with restless legs syndrome.*

conduction velocity but absent sensory nerve conduction in the sural nerve. Light and electron microscopic investigation of a sural nerve biopsy revealed a moderate decrease in density of myelinated fibers, signs of chronic axonal atrophy, especially of large diameter fibers, and a few clusters of small regenerated and remyelinated fibers. Unmyelinated fibers showed no pathology. Muscle biopsy of the soleus muscle revealed both signs of chronic reinnervation (type grouping) and secondary denervation (large group atrophy).

Friedreich's ataxia and neuroacanthocytosis were excluded by genetic analysis and hematological examination. DNA mutation analysis showed increased CAG trinucleotide repeat numbers (n = 53) at the MJD/SCA3 locus on one allele. The other allele was normal.

The proband's siblings II-1 (age 67) AND II-9 (age 50) also fulfilled the criteria for RLS,[9] and both have alleles with 53 repeats. II-9 shows generalized fasciculations, II-1 only few and far between. Apart from an absent Achilles tendon reflex left in subject II-1 and an extensor toe response in the left leg and subclinical 6 to 7 Hz tremor on EMG in II-9, no further abnormalities were found on clinical examination or MRI. The proband's sister (II-5, age 65; 21, and 23 repeats) and his son (III-1, age 43; 54 repeats) experience unpleasant sensations in the calves but do not fulfill the criteria for RLS[9] because the sensations were not worse at rest or in the evening/night and did not improve with movement. Nobody was treated with neuroleptics. Levodopa was not prescribed in the other family members with RLS. It was ineffective in subject II-5. The proband's other siblings and children are healthy and have normal repeat numbers. The proband's father died at the age of 42 suffering from a progressive neurological movement disorder, but unfortunately no further details are available.

Discussion

We describe four members of a family with intermediate CAG repeat numbers of 53 or 54 in the MJD/SCA3 gene. These alleles fall clearly within the inter-

Table. Clinical and Electroneurophysiologal Abnormalities in Subjects with Intermediate Repeat Length MJD/SCA3

Subject	Sural AMPL	Sural NCV	Peroneal AMPL	Peroneal NCV	H-RFL LAT	Median AMPL	Median NCV	EMG SP	EMG MUP	EMG FAS	Full Clinical Picture
	μV	m/s	mV	m/s	ms	mV	m/s				
II-1	7	44	3.4	36	37	5	47	+	+		Pnp, fas, RLS
II-2	ne	ne	2	17	38	14	51	++	+	+	Atx, park, trem, pyr, atrophy, pnp, fas, RLS
II-9	2.5	38	2.5	43	33	10	61	+	+	++	Pyr, trem, pnp, fas, RLS
III-1	11	46	16	49	ne	18	55	Normal			RLS-incomplete
Normal	>5	>40	>5	>40	<35	>10	>50				

Electroneurophysiological values are mean of left and right side.
AMPL = amplitude; NCV = nerve conduction velocity; H-RFL = H-Reflex; LAT = latency; SP = fibrillations and positive sharp waves; MUP = motor unit potentials with long duration and increased amplitude; ne = not evokable; fas = fasciculations; pnp = polyneuropathy; RLS = restless legs syndrome; atx = ataxia; park = parkinsonism; trem = tremor; pyr = pyramidal signs.

mediate range from 45 to 60 between normal and disease alleles. The increase from a 53 to the 54 repeat allele in the youngest generation may indicate that these intermediate alleles are unstable during transmission. Such instability may result in anticipation and hence in, for example, an earlier age at onset or a more severe phenotype.

The proband (II-2) suffers from a late onset, slowly progressive disorder of the spinocerebellar, extrapyramidal, and peripheral nervous system accompanied by RLS. Two other siblings (II-1 and II-9) with intermediate repeat lengths also suffer from RLS and fasciculations. There are two subjects with RLS-like complaints who do not, however, fulfill RLS criteria: the proband's sister (II-5) who has normal alleles, and the proband's son (III-1) who has an allele with 54 repeats. Thus, all those with an intermediate repeat length suffer at least from RLS and fasciculations, except the youngest one, the proband′s son, who is 43 years old but who is probably at risk of RLS in the future because the penetrance of the gene abnormality before the age of 50 is probably less than 100%.[10]

Our family shows that intermediate repeat lengths in the MJD/SCA3 gene can cause both central and peripheral nervous system dysfunction, which may present with RLS, fasciculations, and polyneuropathy only. The clinical signs, nerve and muscle biopsy, nerve conduction studies, and EMG best fit a primary axonal polyneuropathy and motoneuron disorder. It has previously been suggested that shorter repeat lengths correlate with more peripheral signs such as polyneuropathy,[11–14] although a direct correlation between the repeat length and the degree of peripheral nerve damage could not be demonstrated.[15] However, because polyneuropathy occurs with equal frequency in most autosomal dominant cerebellar ataxias, but RLS only in MJD/SCA3, a central effect must be involved in RLS in MJD/SCA3.[8] This is in accordance with the general notion that RLS is caused by an impairment of the dopaminergic system and that peripheral nerve damage may alter CNS neurotransmitter function, thereby predisposing to RLS.[16,17] Both abnormalities are probably present in a majority of MJD/SCA3 patients, which may explain why especially these patients are at risk for RLS. There is further evidence that intermediate MJD/SCA3 alleles may cause a disorder of the peripheral nervous system. Two previous reports describe patients with 54 and 56 repeats, suffering respectively from an axonal polyneuropathy, and autonomic neuropathy with ataxia.[6,7] Furthermore, animal experiments show that an intermediate repeat length (n = 49) can induce the formation of intranuclear cellular inclusions consisting of the abnormal gene product ataxin-3, thereby causing damage at the cellular level, whereas a normal repeat length (n = 27) does not.[18] However, the truncated protein had a smaller chance of forming inclusions than a full-length ataxin-3.[18]

Whether intermediate repeat lengths predispose to a peripheral nervous system disorder, or whether both the central and peripheral nervous system are equally involved but the peripheral disorder is more easily noticed, remains to be elucidated.

References

1. Andrew SE, Goldberg YP, Hayden MR. Rethinking genotype and phenotype correlations in polyglutamine expansion disorders. Hum Mol Genet 1997;6:2005–2010.
2. Sinden RR. Biological implications of the DNA structures associated with disease-causing triplet repeats. Am J Hum Genet 1999;64:346–353.
3. Onodera O, Idezuka J, Igarashi S, et al. Progressive atrophy of cerebellum and brainstem as a function of age and the size of the expanded CAG repeats in the MJD1 gene in Machado-Joseph disease. Ann Neurol 1998;43:288–296.
4. Rosenberg RN. Joseph disease: an autosomal dominant motor system degeneration. In: de Jong JN, ed. Handbook of clinical neurology. Rev. series. Hereditary neuropathies and spinocerebellar atrophies. Vol. 16. New York: Elsevier, 1991:467–479.
5. Lopes-Cendes I, Silveira I, Maciel P, et al. Limits of clinical assessment in the accurate diagnosis of Machado-Joseph disease. Arch Neurol 1996;53:1168–1174.
6. van Schaik IN, Jobsis GJ, Vermeulen M, et al. Machado-Joseph disease presenting as severe asymmetric proximal neuropathy. J Neurol Neurosurg Psychiatry 1997;63:534–536.
7. Takiyama Y, Sakoe K, Nakano I, Nishizawa M. Machado-Joseph disease: cerebellar ataxia and autonomic dysfunction in a patient with the shortest known expanded allele (56 CAG repeat units) of the MJD1 gene. Neurology 1997;49:604–606
8. Schöls L, Haan J, Riess O, et al. Sleep disturbance in spinocerebellar ataxias. Is the SCA3 mutation a cause of restless legs syndrome? Neurology 1998;51:1603–1607.
9. Walters AS. Toward a better definition of the restless legs syndrome. The International Restless Legs Syndrome Study Group. Mov Disord 1995;10:634–642.
10. Higgins JJ, Nee LE, Vasconcelos O, et al. Mutations in American families with spinocerebellar ataxia (SCA) type 3: SCA3 is allelic to Machado-Joseph disease. Neurology 1996;46:208–213.
11. Maruyama H, Kawakami H, Kohriyama T, et al. CAG repeat length and disease duration in Machado-Joseph disease: a new clinical classification. J Neurol Sci 1997;152:166–171.
12. Yoritaka A, Nakagawa-Hattori Y, Hattori N, et al. A large Japanese family with Machado-Joseph disease: clinical and genetic analysis. Acta Neurol Scand 1999;99:241–244.
13. Kubis N, Durr A, Gugenheim M, et al. Polyneuropathy in autosomal dominant cerebellar ataxias: phenotype-genotype correlation. Muscle Nerve 1999;22:712–717.
14. Soong BW, Lin K. Correlation of peripheral nerve fiber loss and trinucleotide repeats in Machado-Joseph disease. Can J Neurol Sci 1998;25:59–63.
15. Klockgether T, Schols L, Abele M, et al. Age related axonal neuropathy in spinocerebellar ataxia type 3/Machado-Joseph disease (SCA3/MJD). J Neurol Neurosurg Psychiat 1999;66:222–224.
16. Chokroverty S, Jankovic J. Restless legs syndrome. A disease in search of an identity. Neurology 1999;52:907–910.
17. Ondo W, Jankovic J. Restless legs syndrome: clinicoetiologic correlates. Neurology 1996;47:1435–1441.
18. Chai Y, Koppenhafer SL, Shoesmith SJ, et al. Evidence for proteasome involvement in polyglutamine disease: localization to nuclear inclusions in SCA3/MJD and suppression of polyglutamine aggregation in vitro. Hum Mol Genet 1999;8:673–682.

Autoantibodies to Amyloid-β and Alzheimer's Disease

Bradley T. Hyman, MD PhD, Carolyn Smith, MA, Ilya Buldyrev, Christa Whelan, BS, Harold Brown, MD, Ming-Xin Tang, PhD, and Richard Mayeux, MD MSc

Immunization against amyloid-β has been suggested as a possible preventive or therapeutic treatment for Alzheimer's disease. We hypothesized that some individuals may have autoantibodies to amyloid-β and that this may be protective. We analyzed the plasma of 365 individuals, drawn from a larger longitudinal epidemiological study, for the presence of antibodies to amyloid-β. There were detectable but very low levels of anti-amyloid-β antibodies in just over 50% of all samples and modest levels in under 5% of all samples. However, neither the presence nor the level of anti-amyloid-β antibodies correlated with the likelihood of developing dementia or with plasma levels of amyloid-β peptide. These data suggest that low levels of anti-amyloid-β autoantibodies are frequent in the elderly population but do not confer protection against developing dementia.

Ann Neurol 2001;49:808–810

Recent data from transgenic mouse models of Alzheimer's disease (AD) suggest that immunization against amyloid-β peptide can prevent subsequent deposition of amyloid plaques.[1] Supportive data show that passive immunization with anti-amyloid-β antibodies also prevents amyloid deposition,[2] that vaccination ameliorates behavioral deterioration in mice,[3,4] and even that existing plaques can be cleared.[5] These observations led us to ask whether individuals in the general population may harbor anti-amyloid-β antibodies, either as a response to having AD or as an incidental phenomenon that may serve a protective role against AD.

Data were included from 365 individuals, selected from a prospective study of 2,126 Medicare recipients, 65 years and older, residing in a single community in northern Manhattan (Table). The cohort was followed

From the Departments of [1]Neurology and [2]Psychiatry, Taub Institute for Research in Alzheimer's Disease and the Aging Brain, Gertrude H. Sergievsky Center, Columbia University College of Physicians and Surgeons, New York, NY, and [3]Alzheimer Disease Research Unit, Massachusetts General Hospital, Charlestown, MA.

Received Feb 21, 2001, and in revised form Mar 23, 2001. Accepted for publication Mar 27, 2001.

Address correspondence to Dr Hyman, Department of Neurology, Harvard Medical School, Alzheimer Research Unit, Massachusetts General Hospital, 114 16th St, Rm 2009, Charlestown, MA 02129. E-mail: B_HYMAN@helix.mgh.harvard.edu

Table. Comparison of Patients with Healthy Elderly

Variable	Alzheimer's Disease	Healthy Elderly	Comment
Number	82 (23%)	271 (77%)	
Age (years)	76.0 (S.D. 7.11)	75.8 (S.D. 5.9)	$F = 0.1$, $p = 0.7$
Women %	64 (78%)	184 (68%)	$\chi^2 = 3.1$, $p = 0.08$
Ethnic group			
African-American	33 (40%)	88 (33%)	
Caribbean Hispanic	40 (49%)	108 (40%)	
Caucasian	9 (11%)	75 (27%)	$\chi^2 = 9.74$, $p = 0.02$
Amyloid-β antibodies	16.07, (S.D. 17.5)	16.96, (S.D. 41.5)	$F = 0.36$, $p = 0.85$

S.D., standard deviation.

over a 7-year period beginning in 1992. Three follow-up examinations took place at 20-month intervals after the baseline interview. Over the study period, the annual mortality rate was 8.1%, the overall refusal rate was 10%, and the annual incidence rate of AD was 3%. Each person had received the same medical, neurological, and neuropsychological evaluations. The study population was randomly selected from individuals who had blood samples and had been followed for at least 4 years with 3 clinical assessments. We excluded anyone with a stroke or parkinsonism or Parkinson's disease. By the last visit, 23% were demented. All were relatively new cases. Of the demented cases, 49% were considered incident cases (those who developed dementia after the baseline interview), and the remainder were prevalent cases (those with dementia at the baseline interview).

We developed an enzyme-linked immunosorbent assay (ELISA) to detect antiamyloid-β immunoreactivity. Amyloid-β 1-42 (10 μg/ml in well-coating buffer; American Peptide) was coated on the odd columns of a Nunc (Naperville, IL) MaxiSorp 96-well plate overnight, then washed. Plates were incubated for 2 hours in blocking solution at 37°C, which was aspirated prior to addition of plasma samples. Plasma samples were sequentially diluted to a final dilution of 1:2,700 along plate columns. After washing 4 times with 1× Tris-buffered saline (pH 7.4) containing 0.05% Tween 20, bound antibody was detected using 1:1,000 anti-human horseradish peroxidase (HRP) secondary antibody. After repeated washing, color was developed for 30 minutes and stopped using 2.5 N sulfuric acid. Color intensity was read at 450 nm. Positive controls of monoclonal antibody 10D5 (Elan Pharmaceuticals), detected using an anti-mouse HRP conjugate, were used to establish a standard curve, and the amount of antibody per microliter was calculated using a 1:300 dilution for all samples. In addition, titers were calculated by evaluating the dilution at which the well containing amyloid-β1-42 had at least 2.1-fold higher signal than the adjacent (uncoated) well.

We found that 192 of the 365 samples analyzed had at least low-level, detectable antiamyloid-β immunoreactivity. This cut-off represents samples with a 2.1-fold higher signal than the uncoated well at 1:300 dilution, corresponding to a concentration of approximately 10 μg/ml. Of the 192 positive samples, 12 had levels greater than 50 μg/ml and 5 had levels greater than 100 μg/ml. These figures correspond to dilution titers of approximately 1:900 in the highest cohort. Thus, it is not uncommon to have low-level antiamyloid-β reactivity in plasma samples.

We next analyzed whether the presence or absence of antibodies or the amount of anti-amyloid-β immunoreactivity impacted either of 2 variables: risk for developing AD and plasma amyloid-β levels. Comparison of amyloid-β titers in the healthy elderly and AD patients revealed no differences (Table). We also compared the 95th percentile of titers to the 5th percentile of titers and found essentially identical risk for AD (35% AD vs. 38.9%, $p = 0.80$). Of the 5 individuals with titers >100 μg/ml, 1 had AD. The average age at onset for individuals with higher titers did not differ from that of individuals with undetectable titers. There was no relationship between titer and amyloid-β 40 or amyloid-β 42 levels, as previously determined.[6] Titers did not vary by gender, age, ethnic group, or APOE genotype. Titers were slightly, but not significantly, higher among individuals who died during follow-up (alive 16.3, standard deviation 38.9, vs. dead 19.9, standard deviation 21.1; $p = 0.5$).

One concern about the clinical use of a vaccination strategy for amyloid-β is that antibodies against an autoantigen may be toxic. Our results show that at least low titers of antibodies that recognize amyloid-β are fairly common in the elderly population, and as such, it is reassuring that no clear toxicity is associated with the presence of anti-amyloid-β immunoreactivity in the plasma. It is important to note that these relatively low titers are less than those obtained in experimental conditions and, for the most part, likely reflect relatively low-affinity interactions, below the level of clinical significance. Nonetheless, low levels of anti-amyloid-β immunoreactivity do not appear to be suffi cient to impact AD risk or amyloid-β concentration in the plasma; clearly, the end point of vaccination trials

will need to be substantially higher levels of titers than those observed herein.

This research was supported by federal grants AG08702 (RM), AG07232 (RM), AG05134 (BH), and AG08487 (BH).

References

1. Schenk D, Barbour R, Dunn W, et al. Immunization with amyloid-beta attenuates Alzheimer-disease-like pathology in the PDAPP mouse. Nature 1999;400:173–177.
2. Bard F, Cannon C, Barbour R, et al. Peripherally administered antibodies against amyloid beta-peptide enter the central nervous system and reduce pathology in a mouse model of Alzheimer disease. Nat Med 2000;6:916–919.
3. Morgan D, Diamond DM, Gottschall PE, et al. A beta peptide vaccination prevents memory loss in an animal model of Alzheimer's disease. Nature 2000;408:982–985.
4. Janus C, Pearson J, McLaurin J, et al. A beta peptide immunization reduces behavioural impairment and plaques in a model of Alzheimer's disease. Nature 2000;408:979–982.
5. Bacskai B, Kajdasz S, Christie R, et al. Imaging of amyloid-β deposits in brains of living mice permits direct observation of clearance of plaques with immunotherapy. Nat Med 2001;7: 369–372.
6. Mayeux R, Tang MX, Jacobs DM, et al. Plasma amyloid beta-peptide 1-42 and incipient Alzheimer's disease. Ann Neurol 1999;46:412–416.

Treatment of Acute Nipah Encephalitis with Ribavirin

Heng-Thay Chong, MRCP,[1]
Adeeba Kamarulzaman, FRACP,[1] Chong-Tin Tan, FRCP,[1]
Khean-Jin Goh, MRCP,[1] Tarmizi Thayaparan, MRCP,[3]
Sree Raman Kunjapan, MRCP,[3]
Nee-Kong Chew, MRCP,[1] Kaw-Bing Chua, FRCP,[2]
Sai-Kit Lam, PhD[2]

Nipah virus, a newly identified paramyxovirus caused a severe outbreak of encephalitis in Malaysia with high fatalities. We report an open-label trial of ribavirin in 140 patients, with 54 patients who were managed prior to the availability of ribavirin or refused treatment as control. There were 45 deaths (32%) in the ribavirin arm; 29 deaths (54%) occurred in the control arm. This represents a 36% reduction in mortality ($p = 0.011$). There was no associated serious side effect. This study suggests that ribavirin is able to reduce the mortality of acute Nipah encephalitis.

Ann Neurol 2001;49:810–813

Between September 1998 and June 1999, an outbreak of encephalitis involving 265 cases and 105 fatalities occurred among pig farm workers in Malaysia. The etiological agent was later identified to be the Nipah virus, a new paramyxovirus.[1–3] The infection was thought to spread from infected pig to man through close contact with body fluid.[4,5] The illness in humans is characterized by severe encephalitis, with distinctive clinical signs such as segmental myoclonus, areflexia, hypertension, and tachycardia.[6] The disease has a rapid onset with death occurring within 10 days of the onset of the illness. Death was probably the result of severe brain-stem involvement.[6] The main pathology was disseminated microinfarctions of the central nervous system from vasculitis-induced thrombosis. Direct neuronal involvement was also thought to be important in the pathogenesis.[7]

Following the identification of the Nipah virus, ribavirin was used in an open-label trial. Ribavirin was selected because of its broad spectrum of activity against

From the Departments of [1]Medicine and [2]Microbiology, University Malaya Medical Centre, Lembah Pantai, Kuala Lumpur, Malaysia; and [3]Department of Medicine, Seremban Hospital, Jalan Rasah, Negeri Sembilan, Malaysia

Received Jan 10, 2001 and in revised form Mar 22. Accepted for publication Mar 28, 2001.

Address correspondence to Prof Tan, Neurology Laboratory, University Malaya Medical Centre, Lembah Pantai, 59100 Kuala Lumpur, Malaysia. E-mail: tlip@pl.jaring.my

both RNA and DNA viruses.[8,9] Clinical efficacy has been shown in haemorrhagic fever with renal syndrome caused by the Hantaan virus and Lassa fever,[10,11] and probable efficacy in respiratory syncytial virus infection.[12] In vitro activity has been demonstrated against West Nile virus[13] and the Hendra virus, another novel paramyxovirus closely related to Nipah virus, with antiviral effect demonstrated at 10 to 50 μg/ml (S. Locarnini, Victorian Infectious Diseases Service, Australia, personal communication). Ribavirin has also been shown to inhibit the replication of Nipah virus by one and a half logs in vitro (Harvey Westbury, Australian Animal Health Laboratory, CSIRO, personal communication). Furthermore, ribavirin was demonstrated to sufficiently cross the blood-brain barrier following oral administration with a mean CSF/plasma ratio of 0.7.[14] This is a report on its use in acute Nipah encephalitis during the outbreak period.

Patients and Methods

Study Population

The patients were from the two main centers that managed most of the patients during the outbreak: Seremban Hospital, a community hospital, and University Malaya Medical Centre, Kuala Lumpur, a tertiary referral center. The patients were treated by a team of internists, neurologists, intensive care physicians, and infectious disease physicians.

Patients were offered ribavirin therapy if they fulfilled the case definition for Nipah encephalitis. Patients were considered to have Nipah encephalitis if they came from known outbreak areas, had direct or close contact with pigs or other infected animals, and had evidence of encephalitis as previously defined.[6,7] The case definition of Nipah encephalitis was based on clinical and epidemiological criteria without requiring a positive serology, as some patients died before seroconversion. The positive serology was seen in only 76% of patients overall.[6] Whereas the median duration of illness to death was 9.0 days, the cumulative 75% seropositive responses was seen at day 15 of illness for serum IgM and day 34 for serum IgG.[15] A case definition based on serology criteria would have underestimated the number of patients with Nipah encephalitis. There were also no differences in the clinical characteristics between patients with and without positive serology and no evidence of a concurrent epidemic of encephalitis due to other agents.[6] Nonetheless, the patients with positive serology were also analyzed separately in this study.

Patients who were managed prior to the availability of ribavirin or refused ribavirin were taken as controls. Table 1 is a comparison between treated and controls. As shown, they shared similar characteristics.

Drug Administration

Ribavirin was available in sufficient quantity by March 19, 1999. All patients who were still in the acute phase of the illness were offered ribavirin. Consent was obtained from the patients or their next-of-kin. All patients were informed of the potential for teratogenicity of ribavirin, and women of child-bearing age were counseled regarding prevention of pregnancy for 6 months.

Ribavirin was given orally 2 g on day 1, 1.2 g tds on days 2 to 4, 1.2g bd on days 5 and 6, 0.6g bd for another 1 to 4 days. The dosing schedule was based on previous trials and the manufacturer's recommendations to achieve a pseudo-steady state concentration of ≈2,500 ng/ml within 24 hours.[10,11] Intravenous ribavirin, which became available during the latter part of the outbreak, was given to patients who were not able to take the medication orally, at a loading dose of 30 mg/kg, then 16 mg/kg every 6 hours for 4 days, and 8 mg/kg every 8 hours for 3 days.

Laboratory Studies

Sera were tested for IgM and IgG antibodies by using an IgM-capture antibody EIA and an indirect EIA, respectively,

Table 1. Patient Characteristics According to Treatment

	All patients			Hendra serology positive		
Characteristic	Ribavirin (n = 140)	Control (n = 54)	p values	Ribavirin (n = 90)	Control (n = 37)	p values
Age (year)	37.8 ± 12.0	38.5 ± 13.9	0.71	36.4 ± 11.3	41.3 ± 14.9	0.48
Sex (percentage of men)	85% (n = 119)	85% (n = 46)	0.88	84% (n = 76)	89% (n = 33)	0.68
Race (percentage of Chinese)	70% (n = 98)	68% (n = 37)	0.92	68% (n = 62)	70% (n = 26)	>0.99
Occupation (percentage of pig farm owners)	50% (n = 69)	49% (n = 26)	0.93	48% (n = 43)	54% (n = 20)	0.65
Diabetes mellitus	4.2% (n = 6)	7.5% (n = 4)	0.46	3.3% (n = 3)	8.1% (n = 3)	0.36
Systolic blood pressure on admission	130 ± 16	138 ± 25	0.046	131 ± 16.4	140 ± 25.5	0.058
Diastolic blood pressure on admission	78 ± 13	84 ± 16	0.015	80 ± 13	85 ± 17	0.068
Temperature on admission	38.0 ± 0.9	38.2 ± 0.9	0.13	38.1 ± 0.8	38.2 ± 0.9	0.44
Heart Rate on admission	86 ± 15	86 ± 19	0.27	86 ± 14	83 ± 19	0.42
Glasgow Coma Scale score on admission (median)	14	13	0.0029	15	14	0.001

against the Hendra virus antigens, which cross-react with Nipah antibodies. Complete blood count and liver function test were performed at baseline and daily until completion of therapy.

Outcome Analysis

The primary outcome was death. Secondary outcomes included residual neurological deficits and the need for mechanical ventilatory support.

Results

A total 194 patients with encephalitis were treated, 103 patients at the Seremban Hospital and 91 patients at the University Malaya Medical Centre. The patient characteristics from the two centers were similar except that there were more ethnic Chinese and pig farm owners from the latter. A total of 140 patients were given ribavirin, and 54 patients served as control. Of the control, 52 patients were managed prior to the availability of ribavirin; 128 patients received oral ribavirin, 12 patients received intravenous ribavirin. The median follow-up period was 336 days (range: 14–528 days), with only 1 patient who did not attend follow-up. There were 74 (38%) deaths, 42 (40%) in Seremban Hospital and 32 (35%) in University Malaya Medical Centre, with no statistically significant difference between the two centers ($p = 0.5$). The median course of illness from the onset of symptoms to death was 9.0 days (range: 2–3/2days).

There were 45 deaths in the treated group (32%) and 29 in the controls (54%), with 36% reduction in mortality. On univariate analysis, hypertension and a lower Glasgow Coma Scale score on admission were significant prognostic factors for mortality ($p = 0.005$ and 0.02, respectively). On Cox regression analysis, younger age and use of ribavirin were independently associated with better survival ($p = 0.011$ and 0.013, respectively). The relative risk of death with ribavirin was 0.72 (95% CI 0.56–0.93). If only those patients with positive Hendra serology were included in the analysis ($n = 127$), the effect of ribavirin on survival is still significant (Table 2). On multivariate regression analysis, patients treated with ribavirin were just as likely to be ventilated as the control and were less likely to have residual neurological deficits at the end of follow-up, though this did not reach statistic significance. On univariate analysis, these patients were ventilated longer, and stayed longer in the hospital when compared to controls (Table 2). On post-hoc analysis, they were also more likely to have septicaemia (18.7% vs. 1.89%).

Common side effects of ribavirin include anaemia, jaundice, and teratogenic effect. There was no significant difference in the incidence of anemia in the treatment group as compared to controls. The ribavirin group however, was more likely to develop abnormally raised serum bilirubin level, although this did not reach statistical significance.

Discussion

This study showed that ribavirin treatment in acute Nipah encephalitis was associated with a 36% reduction in mortality and more survivors without neurological deficits, although the latter did not achieve statistical significance. The beneficial effect of ribavirin was also significant among those with positive Hendra serology. We compared patients who were treated with ribavirin with patients who were managed before the availability of ribavirin therapy and those who refused treatment with ribavirin. Both sets of patients came from the same outbreak areas and were managed by the same teams of medical personnel in the respective centers. There was no difference in the severity of the disease in the two groups with the proportion of patients requiring ventilation being similar. Yet there was a demonstrable difference in mortality and good survival between the two groups.

Table 2. Effect of Ribavirin

	All patients			Hendra serology positive		
Outcome	Ribavirin (n = 140)	Control (n = 54)	p values[b]	Ribavirin (n = 90)	Control (n = 37)	p values[b]
Mortality	32% (n = 45)	54% (n = 29)	0.011	26% (n = 23)	54% (n = 20)	0.0057
Ventilation	57% (n = 80)	54% (n = 29)	0.14	59% (n = 53)	60% (n = 22)	0.95
Survivors without deficits	52% (n = 73)	41% (n = 22)	0.17	60% (n = 54)	38% (n = 14)	0.16
Duration of ventilation, days	9.4 ± 8.7	4.2 ± 2.4	0.0002	10.1 ± 9.2	3.8 ± 1.9	0.001
Duration of stay, days	23.7 ± 27.6	11.7 ± 6.4	<0.0001	24.7 ± 32.6	7.3 ± 5.5	0.001
Anemia[a]	37% (n = 52)	37% (n = 20)	0.89	39% (n = 35)	49% (n = 18)	0.50
Bilirubin, μmol/l	21.7 ± 1.9	13.4 ± 1.6	0.11	22.7 ± 16.2	14.8 ± 5.0	0.24

[a]Hemoglobin < 13.5 g percent for male and <11.5 g percent for female.
[b]Statistical analysis was performed with ANOVA for univariate parametric variables, while χ^2 or Fisher's exact test were used for univariate nonparametric variables. The primary and secondary outcomes were analyzed by Cox and logistic regression analyses.

The fact that the treated group was ventilated longer, was more likely to have septicemia, and had a longer duration of stay in the hospital was also consistent with the beneficial effect of ribavirin, with the increase in the number of survivors.

Most of the patients in the study were given oral ribavirin. Intravenous ribavirin was only given to a few patients in the latter part of the outbreak, as it was not initially available. A comparison of the effect of intravenous versus oral ribavirin cannot be made because of the small number of patients treated intravenously. Previous studies have shown the mean systemic availability of oral ribavirin to be approximately 42%.[14]

The study, however, suffered from the drawback associated with the use of historical controls. As the outbreak was associated with a disease that was not previously recognized, it was possible that during the latter part of the outbreak when ribavirin was introduced, the treating physicians were also more skillful in the general management of the patients. The beneficial effect of ribavirin should thus be confirmed with a randomized placebo-controlled trial.

We thank the Minister and Director-General of the Ministry of Health, Malaysia, for the generous provision of rivabirin; Dr. Thomas Ksiazek and his team from the Centers of Disease Control and Prevention for their help in the serological tests; the doctors and nurses from the Special Wards 3A, 3B, the Intensive and Coronary Care Units, Seremban Hospital and Wards 2T, 6E and 9B at the University Malaya Medical Centre for the dedicated care of patients.

References

1. Outbreak of Hendra-like virus—Malaysia and Singapore, 1998–1999. MMWR Morb Mortal Wkly Rep 1999,48;265–269.
2. Chua KB, Goh KJ, Wong KT, et al. Fatal encephalitis due to the Nipah virus among pig-farmers in Malaysia. Lancet 1999; 354:1257–1259.
3. Chua KB, Bellini WJ, Rota PA, et al. Nipah virus: a recent emergent deadly Paramyxovirus. Science 2000;288:1432–1435.
4. Parashar UD, Lye MS, Ong F, et al. Case-control study of risk factors for human infection with a new zoonotic paramyxovirus, Nipah virus, during a 1998–1999 outbreak of severe encephalitis in Malaysia. J Infect Dis 2000;181:1755–1759.
5. Tan KS, Goh KJ, Tan CT. Epidemiological aspects of Nipah virus infection. Neurol J Southeast Asia 1999;4:77–81
6. Goh KJ, Tan CT, Chew NK, et al. Clinical features of Nipah virus encephalitis among pig farmers in Malaysia. N Eng J Med 2000;342:1229–1235.
7. Chua KB, Lam SK, Tan CT, et al. High mortality in Nipah encephalitis is associated with presence of virus in cerebrospinal fluid. Ann Neurol 2000;48:802–805.
8. Lin OS, Keeffe EB. Current treatment strategies for chronic hepatitis B and C. Annu Rev Med 2001;52:29–49.
9. Huggins JW. Prospects for treatment of viral haemorrhagic fevers with ribavirin, a broad-spectrum antiviral drug. Rev Infect Dis 1989;ii:S750–761.
10. Huggins JW, Hsiang CM, Cosgriff TM, et al. Prospective, double-blind, concurrent,placebo-controlled clinical trial of intravenous ribavirin therapy of haemorrhagic fever with renal syndrome. J Infect Dis 1991;164:1119–1127.
11. McCormick JB, King IJ, Webb PA, et al. Lassa fever. Effective therapy with ribavirin. N Engl J Med 1986;314:20–26.
12. Rodriguez WJ, Hall CB, Welliver R, et al. Efficacy and safety of aerosolized ribavirin in young children hospitalized with influenza; A double-blind, multicenter, placebo-controlled trial. J Pediatr 1994;125:129–135.
13. Jordan I, Briese T, Fisher N, et al. Ribavirin inhibits West Nile virus replication and cytopathic effect in neural cells. J Infect Dis 2000;182:1214–1217.
14. Connor E, Morrison S, Lane J, et al. Safety, tolerance, and pharmacokinetics of systemic ribavirin in children with human immunodeficiency virus infection. Antimicrob Agents Chemother 1993;37:532–539.
15. Ramasundrum V, Tan CT, Chua KB, et al. Kinetics of IgM and IgG seroconversion in Nipah virus infection. Neurol J Southeast Asia 2000;5:23–28.

Right Lateralized Motor Cortex Activation During Volitional Blinking

Thilo van Eimeren, cand med,[1] Henning Boecker, MD,[2] Elisabete Castelon Konkiewitz, MD,[1] Markus Schwaiger, MD,[2] Bastian Conrad, MD,[1] and Andrés O. Ceballos-Baumann, MD[1]

Using $H_2{}^{15}O$ positron emission tomography in 6 healthy volunteers, we found that self-initiated and externally cued blinking activated the right primary motor cortex and supplementary motor area (SMA). The left dorsolateral prefrontal cortex (DLPFC) and the rostral SMA showed greater activation during the self-initiated task compared to the externally cued task. This study confirms the hypothesis of right hemispheric lateralization of volitional blinking derived from observations in stroke patients. Furthermore, it underscores the role of DLPFC and rostral SMA in self-initiated movements, which has been found in similar experiments with hand movements.

Ann Neurol 2001;49:813–816

Blinking is a universal motor phenomenon, which is affected in various neurological disorders. Central reg-

From the Departments of [1]Neurology and [2]Nuclear Medicine, Klinikum rechts der Isar, Technische Universität München, Munich, Germany.

Received Jan 23, 2001, and in revised form Mar 19. Accepted for publication Mar 28, 2001.

Published online 25 May 2001.

Address correspondence to PD Dr Ceballos-Baumann, Neurologische Klinik der TUM, Klinikum rechts der Isar, Möhlstrasse 28, D-81675 Munich, Germany. E-mail: a.ceballos@lrz.tu-muenchen.de

ulation of blinking involves cortex, extrapyramidal motor systems, and rostral brainstem structures.[1] Observations in stroke patients have implicated a number of cortical regions, including parietal and frontal lobe, especially the supplementary motor area (SMA)[2] and frontal area 8[3], but also parts of the temporal and occipital lobes.[2–5] The clinical finding that unilateral lesions impairing volitional eyelid function are practically always on the right side provides grounds for supposing dominance of the right hemisphere.[1,2,4]

The current concept of motor cortical representation has been influenced greatly by Penfield's homunculus.[6] However, in the original publications, the cerebral cartography of eyelid blinking has not been very precise. Indeed, electrical stimulation over approximately two-thirds of the precentral gyrus elicited eyelid movements, and the authors could not state whether the movements were mainly contra- or mainly bilateral, because ". . . the ipsilateral eye could not be seen because of the sterile sheets with which the patient was draped."[6]

The aim of the present study was to identify the functional anatomy of human volitional blinking using $H_2{}^{15}O$ positron emission tomography (PET). We hypothesized, first, that volitional blinking would activate predominantly the SMA and the right motor cortex, along with areas activated in other motor tasks (premotor cortex, basal ganglia, cerebellum, insula, and midbrain structures), based on previous functional imaging studies and the clinical evidence of supranuclear eyelid movement disorders[2,4,5,7,8] and, second, that internally vs externally cued blinking would be associated with an increased activation of rostral SMA and dorsolateral prefrontal cortex (DLPFC), similarly to findings in hand motor paradigms.[7,8]

Subjects and Methods

Subjects

We studied a group of 6 healthy volunteers (3 female, 3 male, mean age 57 ± 5.6 years, range 51–72 years) with $H_2{}^{15}O$ PET. Eye blinks were monitored by surface electromyograph (EMG), which was used to initiate a tone in the task of self-initiated blinks (see below).

Tenets of the Declaration of Helsinki were followed, and written informed consent was obtained from all subjects. The experiments were approved by the responsible Ethics Committee, and permission to administer radioactivity was obtained from the radiation safety authorities. All subjects were right-handed according to a modified version of the Edinburgh Handedness Inventory.[9]

Task Conditions

The PET scan was performed in complete darkness; noise such as that from computer ventilators was reduced to a minimum. The paradigm consisted of four blocks with three experimental conditions in a fixed order.

Table. Areas and Coordinates for the Maxima of Increases in Regional Cerebral Blood Flow

Area Activated	x	y	z	Z score
Self-initiated vs rest				
SMA	−4	−2	66	6.00
Auditory association cortex (L)	−64	−36	20	4.44
Visual association cortex	−16	−90	36	4.39
Insula (R)	40	8	8	4.34
Mesencephalon (L)	−14	−24	−8	4.09
Vermis	6	−72	−6	3.97
M1 (R)	48	−4	48	3.60
Externally cued vs rest				
SMA	−4	−4	66	5.03
M1 (R)	46	−4	50	4.64
Insula (R)	34	2	2	4.52
Mesencephalon (L)	−16	−30	−8	4.33
Visual association cortex	−4	−82	16	4.01
Self-initiated vs externally cued				
Visual association cortex	8	−78	−6	3.87
Lateral premotor cortex (L)	−62	6	14	3.15
DLPFC (L)	−38	42	26	3.00
Rostral SMA	−4	4	70	2.94

x And z coordinates are relative to the intercommissural line (negative x values are left hemisphere), and y coordinates are relative to anterior commissure.

SELF-INITIATED BLINKS. Subjects were told to make bilateral fast and complete eyelid closures (blinks) at a comfortable rate. To control for the tone effect in the triggered condition, a tone was presented on average 38 ± 60 msec after each blink. This was accomplished using the suprathreshold EMG signal produced by every blink to induce the tone.

EXTERNALLY CUED BLINKS. Subjects were told to produce the same movements as in the self-initiated condition in response to tones, which we randomized chronologically (±20% of medium interval) to control for anticipation. The medium interval was adjusted to the medium interval in the self-initiated condition to guarantee a balance of movement between the two motor tasks.

REST. Subjects were told to relax and to leave their eyes closed. Tones, which the subjects were told to ignore, were presented with the same medium interval as in the externally cued condition.

During both activation conditions, blinking was monitored with analogue data coming from surface EMG of the orbicularis oculi and was digitized to 12-bit resolution using a CED-1401 general-purpose laboratory interface (Cambridge Electronic Design, Cambridge, United Kingdom). Data collection was controlled using the SigAvg program (version 6.33; Cambridge Electronic Design). For data evaluation, the Spike2 program (version 4.07; Cambridge Electronic Design) was used.

PET Imaging and Analysis

The data acquisition of the regional distribution of radioactivity was performed in three-dimensional (3D) mode with a Siemens 951R/31 PET camera (CTI, Knoxville, TN), with a

total axial field of view of 10.5 cm and no interplane dead space. The data set common to all subjects extended axially from 8 mm below to 70 mm above the intercommissural line. This field of view included both the mesencephalon and the top of the SMA. Most of the cerebellum was outside the field of view. To measure regional cerebral blood flow (rCBF), 7.5 mCi $H_2{}^{15}O$ were administered intravenously over 30 seconds with a semibolus injection using an infusion pump. Single frames were acquired for 60 seconds, starting with the appearance of the tracer in the brain. For further details on the local PET scanning technique and data analysis, we refer the reader to previous work from the authors[10] and from the developers of statistical parametric mapping software (Wellcome Department of Cognitive Neurology, London, United Kingdom).[11] The latest version of SPM99 was used. Significance was accepted when voxels survived a corrected threshold of $p < 0.05$ in areas unpredicted by the hypothesis; voxels with an uncorrected threshold of $p < 0.001$ were accepted when changes were predicted in the area (see introductory section).

Results

Motor Performance

The mean blink frequency across the whole group was 0.73 ± 0.15 Hz (range 0.38–1.10 Hz), that of self-initiated blinks 0.74 Hz, and that of externally cued blinks 0.73 Hz.

Areas of Cerebral Activation

The areas of significant activation relative to rest and the increases in rCBF in the comparison self-initiated vs externally cued are shown in the Table and in the Figure.

SELF-INITIATED BLINKS VS REST. This comparison was associated with relative rCBF increases in bilateral SMA, right primary motor cortex (M1), right insular cortex, vermis, and left mesencephalon. Increased rCBF occurred in that part of the vermis included in the field of view.

EXTERNALLY CUED BLINKS VS REST. This comparison was associated with relative rCBF increases in bilateral SMA, right M1, right insular cortex, and left mesencephalon.

SELF-INITIATED VS EXTERNALLY CUED BLINKS. Increased rCBF occurred in rostral SMA and left DLPFC (for the a priori hypothesis, see introductory section), but the increase was just below the chosen statistical threshold ($p = 0.002$).

Other cortical areas with an uncorrected threshold of $p < 0.001$ not predicted a priori are listed in the Table.

Discussion

This is the first study showing right lateralized motor cortex activation during volitional blinking, which was suggested by clinical observations in stroke patients.[2,4,5] These reports describe in particular the inability of such patients to close or open the eyes on command, whereas spontaneous blinking and reflex blinking are preserved.[2,4] The activation cluster observed on the precentral gyrus is focal compared to approximately two-thirds of the precentral gyrus that elicited eyelid movements in the early somatotopic mapping experiments.[6] The peak of the activation cluster is situated almost at the same level relative to the anterior-posterior commissural (AC-PC) line as the foci for finger, fist, and hand opposition movements found

Fig. PET activation increases superimposed on 3D-rendered brain. View from above, and right hemisphere on the right side. A = self-initiated vs rest; B = externally cued vs rest; C = self-initiated vs externally cued.

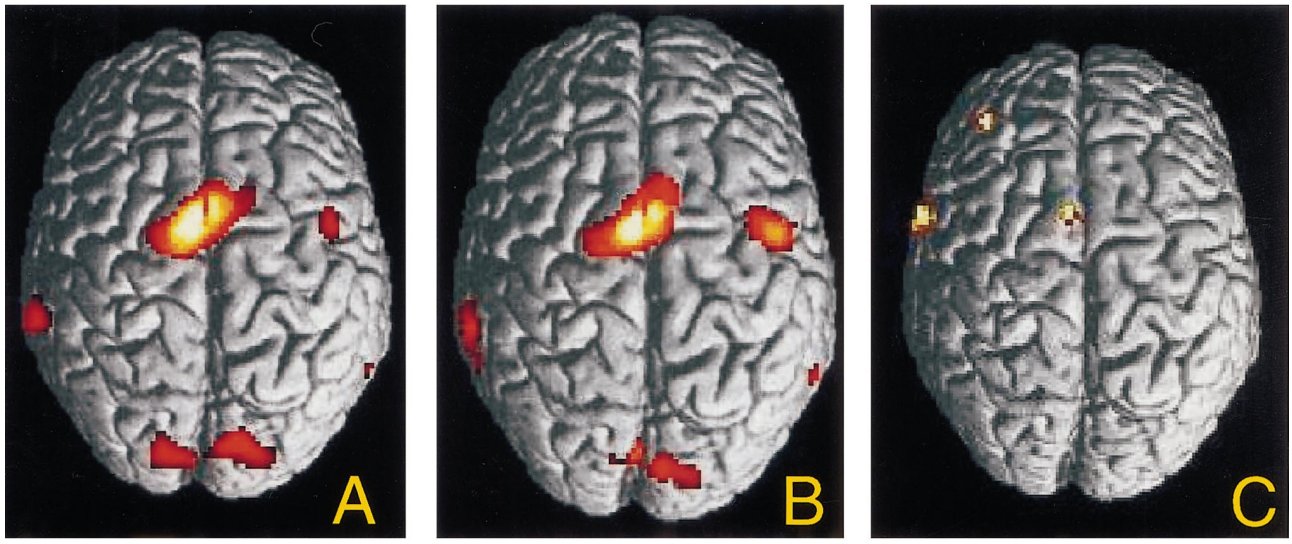

in previous PET studies.[12,13] Whereas other axial movements such as swallowing are associated with bilateral activation of more inferior parts of the precentral gyrus, blinking shows a strong lateralization to the right.[14]

Previous functional imaging studies that involved voluntary eye blinking in their activation paradigms did not report motor cortex or SMA activation. The reason for this divergence lies in differences in field of view, paradigm, and technology. Bodis-Wollner et al.[15] evaluated with functional magnetic resonance imaging (fMRI) whether the same or different cortical areas participate in voluntary blinks and in voluntary saccades. They obtained only five oblique transverse sections and reported parallel activation of frontal, supplementary, and parietal "eye field" as well as visual cortex associated with saccades and blinks. Another fMRI study using single case analysis concluded that blinking "appears to be controlled in the orbitofrontal cortex."[16] These workers do not comment on why blinking should not activate regions classically associated with the motor system. Blaxton et al.[17] and Schreurs et al.[18] studied eye blink conditioning, which makes their studies difficult to compare. Moreover, the field of view they used did not include upper parts of the frontal lobe.

Activation of the SMA was predicted in particular for the self-initiated blinks, and the strength of activation is remarkable for such a simple movement, especially for the externally cued condition. Current concepts of premotor function attribute a particular role of the SMA to the control of internally generated movements, whereas externally generated movements appear to be controlled by lateral premotor areas.[19] Self-initiated vs externally cued eye blink was associated with relative activation increases in rostral SMA and left DLPFC. This proves that recent findings with simple finger movements can be extended to other types of movements, as is shown with our bilateral and axial tasks.[8]

This study was supported by DFG grant Ce 33/4-1.

We thank our subjects for participating in the study and the staff at the PET unit for their help in scanning.

References

1. Schmidtke K, Büttner-Ennever JA. Nervous control of eyelid function. Brain 1992;115:227–247.
2. Colombo A, De Renzi E, Gilbertoni M. Eyelid movement disorders following unilateral hemispheric stroke. Ital J Neurol Sci 1982;1:25–30.
3. Cogan DG. Supranuclear connections of the ocular motor system: lid movements. In: Neurology of the ocular muscles. Springfield, IL: D.G. Cogan, 1974:139–148.
4. Lepore FE. Bilateral cerebral ptosis. Neurology 1987;37:1043–1046.
5. Nutt JG. Lid abnormalities secondary to cerebral hemisphere lesions. Ann Neurol 1977;1:149–151.
6. Penfield W, Rasmussen T. The cerebral cortex of man. New York: Macmillan, 1952.
7. Jahanshahi M, Jenkins IH, Brown RG, et al. Self-initiated versus externally triggered movements I. An investigation using measurement of regional cerebral blood flow with PET and movement-related potentials in normal and Parkinson's disease subjects. Brain 1995;118:913–933.
8. Jenkins IH, Jahanshahi M, Jueptner M, et al. Self-initiated versus externally triggered movements II. The effect of movement predictability on regional cerebral blood flow. Brain 2000;123:1216–1228.
9. Oldfield RC. The assessment and analysis of handedness: the Edinburgh inventory. Neuropsychologia 1971;1(9):97–113.
10. Boecker H, Ceballos-Baumann AO, Bartenstein P, et al. Sensory processing in Parkinson's and Huntington's disease. Investigations with 3D $H_2{}^{15}O$-PET. Brain 1999;122:1651–1665.
11. Frackowiak RSJ, Friston KJ. Functional neuroanatomy of the human brain: positron emission tomography—a new neuroanatomical technique. J Anat 1994;184:211–225.
12. Colebatch JG, Deiber MP, Passingham RE, et al. Regional cerebral blood flow during voluntary arm and hand movements in human subjects. J Neurophysiol 1991;65:1392–1401.
13. Grafton ST, Woods RP, Mazziotta JC. Within-arm somatotopy in human motor areas determined by position emission tomography imaging of cerebral blood flow. Exp Brain Res 1993;95:172–176.
14. Zald DH, Pardo JV. The functional neuroanatomy of voluntary swallowing. Ann Neurol 1999;46:281–286.
15. Bodis-Wollner I, Bucher SF, Seelos KC. Cortical activation patterns during voluntary blinks and voluntary saccades. Neurology 1999;53:1800–1805.
16. Tsubota K, Kwong KK, Lee T, et al. Functional MRI of brain activation by eye blinking. Exp Eye Res 1999;69:1–7.
17. Blaxton TA, Zeffiro TA, Gabrieli JDE, et al. Functional mapping of human learning: a position emission tomography activation study of eyeblink conditioning. J Neurosci 1996;16:4032–4040.
18. Schreurs BG, McIntosh AR, Bahro M, et al. Lateralisation and behavioral correlation of changes in regional cerebral blood flow with classical conditioning of the human eyeblink response. J Neurophysiol 1997;77:2153–2163.
19. Passingham RE. The frontal lobes and voluntary action. Oxford Psychology Series 21. Oxford: Oxford University Press, 1993.